Delft University of Technology

Design framework for mechanically intelligent bio-inspired grasper

Changoski, Vasko; Domazetovska Markovska, Simona; Jovanova, Jovana

Important note
To cite this publication, please use the final published version (if applicable).
Please check the document version above.

TECHNICAL PAPER

Design framework for mechanically intelligent bio-inspired grasper

Vasko Changoski[1] · Simona Domazetovska Markovska[1] · Jovana Jovanova[2]

Abstract

The challenge of designing real-world robots continues due to the complexities of navigating inaccessible terrains and encountering unexpected conditions. Introducing smart materials like shape memory alloys (SMAs) in the robot body can be beneficial due to their shape memory effect for actuation; however, there is no systematic way to introduce SMAs in a robot design. This research aims to address these challenges by proposing a design framework for SMA-actuated smart structures in robotic applications. Drawing inspiration from nature, the initial step in this framework involves conceptualizing a multifunctional grasper. This grasper utilizes SMA springs actuated by electric current, enabling various movements such as crawling, grasping, and folding. Analytical modeling is employed to determine the necessary characteristics of the SMA springs for one segment of the grasper. A multi-body modeling approach is utilized for more comprehensive understanding of the robot performance. This approach verifies the results of the analytical modeling and allows for performance optimization. Grasper's dynamics is enhanced by fine-tuning actuation input signals, resulting in a more precise, sustainable, and energy-efficient grasper that is capable of traveling 400% longer distance than the initial concept design. The conducted experiments confirm that the proposed design framework for mechanically intelligent grasper has the potential to streamline the SMA-actuated structure design process by reducing development time, minimizing the trial-and-error iterations, and yielding cost savings in both development and prototyping phases.

Keywords Multifunctional structure · Design framework · Bio-inspired · SMA materials · Optimization

1 Introduction

Flexible robots have emerged as versatile and adaptive systems to various environments with the potential to execute wide range of real-world tasks. Demonstration of various remarkable capabilities in flexible robots has been shown as jumping [1], crawling [2], adaptable grasping [3], flying [4], and self-morphing and growing [5]. Multifunctional design aims to combine various locomotion modes to create robots capable of performing multiple tasks or functions effectively, using the same design. The goal of incorporating multifunctionality in locomotion is to create more versatile and resource-efficient systems that can handle a wider range of tasks or movements without the need for specialized devices for each function. This approach is particularly valuable in the field of flexible robotics, where optimizing movement capabilities and adaptability are crucial for practical real-world applications.

Multifunctional design can draw inspiration from nature to incorporate diverse and efficient features into a single, unified system. Inspired by animals with modular structures and repetitive movements across their bodies, researchers have explored multi-locomotion systems of bio-inspired robotics [6]. Analysis of multi-locomotion in bio-inspired structures has been conducted in various environments, including air, water and ground [7]. For instance, the development of a bio-inspired multilegged soft millirobot functioning in both dry and wet conditions has demonstrated exceptional locomotion and deformability, heavy carrying capability,

---

Technical Editor: Marcelo A. Savi.

✉ Jovana Jovanova
  J.Jovanova@tudelft.nl

  Vasko Changoski
  vasko.changoski@mf.edu.mk

  Simona Domazetovska Markovska
  simona.domazetovska@mf.edu.mk

1 Faculty of Mechanical Engineering, Ss. Cyril and Methodius University in Skopje, Skopje, Republic of North Macedonia

2 Faculty of Mechanical, Maritime and Materials Engineering, Delft University of Technology, Delft, The Netherlands

Springer

efficient locomotion, over-obstacle ability, and high adaptability [8]. The integration of multiple tapered feet with soft materials has proven to be general and powerful strategy for soft robot development, with potential applications in untethered manipulation, movable laminated sensing, as well as in vivo medical transportation. Another example of bio-inspired robotics is an eight-arm soft robot inspired by the octopus, which can walk in water using similar strategy by exhibiting good performance over various surfaces and grasping objects of different sizes and shapes due to its soft arm materials and conical shape [9].

To further enhance the bio-inspired multifunctional movement design, researchers have explored novel technologies, such as smart materials [10]. The use of shape memory alloy (SMA) as an unconventional actuation method allows for transforming non-mechanical energy into mechanical work to establish various motions, enabling flexibility and multi-locomotion [11]. Integrating different compositions of smart materials in a single monolithic structure during fabrication provides tailored compliant mechanism designs with beneficial behavior [12]. Smart material actuation has been applied to create multi-locomotion robots capable of performing several movements [13].

In addition to smart materials, additive manufacturing (AM) has revolutionized the rapid fabrication of customized components, offering sophisticated and state-of-the-art technologies and materials for robot manufacturing [14]. With the emergence of 3D printing, the produced materials are also being considered and engineered for specific applications. With the employment of AM, different shapes enabling effectiveness could be designed. The AM technologies are focused both on creating objects and enhancing their properties (e.g., strength, versatility, and deformability) [15]. With 3D printing, researchers have been able to design printed materials with shapes that enhance effectiveness, leading to unique structures like self-folding and shape-changing graspers [16] and soft underwater grippers [17].

Flexible robotics spans over wide range of applications, from strawberries harvesting [18], autonomous legged robot for extreme environments exploration [19], and exploration in subterranean environments [20]. In addition, the modular robots have the advantage showing cost-effectiveness through homogeneous design for mass production and simplified maintenance, increased adaptability to diverse tasks and environments, and sensitive robustness with selective replacement of damaged units [21]. The current modular robots achieve basic configurations and tasks, imposing advanced development for high performance [22]. The researchers in [23] merged small soft robots and the demand for safe human-sized robots by introducing a novel soft robotic module and presenting various configurations of human-scale robots built upon this module. The novel technologies including deep reinforcement learning [24] and automated synthesis [25] are used for control of these robots. SMA springs represent key components for actuators that can operate automatically by temperature change [26]. Their usage can be expanded in different research fields such as systems that can withstand severe earthquakes [27] and vibration reduction systems [28].

Multi-body dynamics analysis has been used to replace the traditional springs in drum washing machine [29] and rubber-based damper in commercial vehicle cab [30]. On the other hand, numerical modeling and simulations have been used to describe the behavior of self-centering energy dissipative brace equipped with SMA materials [31] and soft SMA planar actuator [32]. PID controllers have been applied for a design of 2 DOF shape memory alloy actuator using SMA springs [33] and SMA combined finger [34].

In previous work [35], an All Terrain Grasper Transport (AT-GT) was developed, a continuous track vehicle designed for rough terrain, featuring an SMA suspension capable of returning to its original shape after deformation. This study focuses on bio-inspired robotic grasper with the potential to be integrated with the AT-GT. Also, the goal of this paper is to utilize the analytical and multi-body modeling advantages with experimental research. Analytical models are developed for three functions of the grasper, such as grasping, crawling and folding. Based on the analytical models for one segment of the grasper and obtained desired SMA characteristics, multi-body modeling followed by an optimization of an entire smart structure was applied. The optimization performed in ADAMS resulted in a more than fourfold increase in the grasper's travel distance per iteration. Initially covering 25 mm, the grasper's travel range extended to 118 mm. To confirm the design framework concept, a 3D-printed grasper was created and tested. The 3D-printed grasper is actuated by conducting electrical current to the SMA springs by power supply of 80 W. The conducted experiments confirm the data from the crawling movement of the optimized multi-body grasper with acceptable deviation in the results. Therefore, we can confirm that the design framework could lead to improvement in the design process of mechanically intelligent bio-inspired structures. The novelty is in the systematic design approach, utilizing the advantages of analytical and multi-body modeling for SMA springs as actuators. The design framework can support designers, engineers and roboticists in the mission to design more agile, sustainable and efficient robots.

2 Shape memory actuation in robotic structures

The use of analytical and multi-body modeling can drastically reduce the time spent on prototyping and trial-and-error testing. As a result, the overall design process becomes more efficient, enabling the creation of enhanced grippers with fewer iterations. Figure 1 shows the proposed model-based design framework for SMA-actuated mechanically intelligent structures.

The design process of the grasper begins with conceptualizing its form and the number of unit cells which is followed by analytical modeling. This analytical phase evaluates the feasibility of achieving the desired multi-locomotion movements based on the proposed design. Additionally, it identifies potential resistance forces that might arise during multi-locomotion. Next, the characteristics of the actuators' springs are defined and integrated into the multi-body modeling. This step aims to assess whether the actuator forces are sufficient to overcome resistance forces and to optimize their activation interval. To enhance the grasper's performance and energy efficiency, the timing of the actuators is optimized, resulting in improved movement and velocity while reducing energy consumption during activation. This comprehensive process aids in determining the optimal characteristics of the springs to be incorporated into the grasper, thereby identifying the most suitable design and optimizing the overall model for enhanced effectiveness. Once the final design is established, it undergoes testing, and all pertinent data are sent back to the multi-body modeling and design concept for review and further system optimization. This iterative approach ensures a thoroughly refined and efficient grasper design.

To further improve exploration activities and overcome difficulties in real-world conditions, the idea is to make a transporter adaptable to any terrain using SMA materials (Ni–Ti springs) and allow for fast traveling.

The SMA springs were chosen because of their shape memory effect, unique characteristic to deform, sustain the deformed state, and return in their original form after temperature change exposure. The transit occurs by changing their crystal structure from martensite to austenite and vice versa. When heated up, the SMA springs start to change from martensitic phase to austenitic phase at a predefined temperature A_s, and the process is completed at temperature A_f. In this research, this phenomenon is used as an actuator force generated by the SMA springs. For the springs that are used in this research paper the transition temperature is $A_f = 65°C$. When cooling down the Ni–Ti springs start to return to their original martensite state at a temperature M_s lower than A_s and finish the transition at temperature M_f. Because the forward phase transformation is endothermic process while the reverse transformation is exothermic process, an energy unbalance occurs. This dissipative phenomenon is known as hysteresis. This leads to different response characteristics of the material and usually is presented and visualized in stress–strain-temperature diagram [36].

The SMA materials are best known for their characteristic to remember their original shape. At lower temperatures, the SMA materials are in their martensite state and their crystal structure is referred as twinned martensite. When mechanical loading with small intensity is applied, the strain remains in its elastic area. For an example if the SMA material is used for SMA springs, then the springs behave as conventional elastic springs. If the mechanical load is increased up to a point when the stress is high enough to cause inelastic strain, a martensite reorientation occurs and the crystal structure is reoriented in detwinned martensite variant. This results in change of the original characteristics of the material, or in this case the SMA spring would be deformed. Upon heating, they transition from detwinned martensite state to
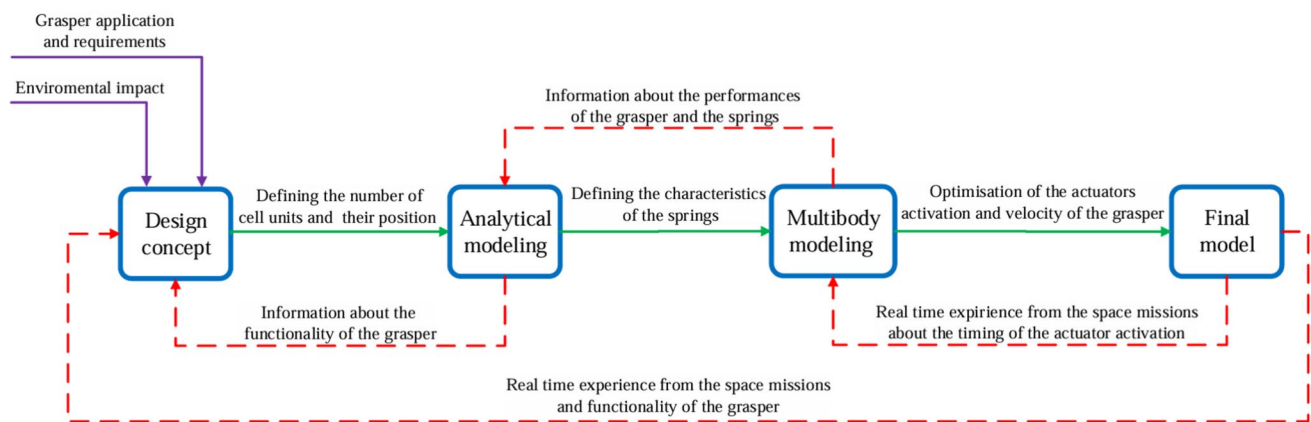

Fig. 1 Flowchart of model-based design framework for SMA-actuated smart structures in grasping robot applications

cubic austenite crystal structure. When the A_f temperature is reached, the SMA spring returns in its original shape. It must be pointed out that the strain caused by the martensite reorientation will be fully recovered when the temperature is near or higher than A_f. When the SMA spring starts the cooling process, then the crystal structure reorientates into the original twinned martensite. This process is known as shape memory effect, and the strain returns to the elastic area [36, 37]. This is easily achieved in the first loading cycles of SMA springs; however, later due to the material fatigue, certain strain becomes non-recoverable.

Beside the SMA spring performances, an analysis of the environment conditions should be considered, especially if there is extreme temperature variation. The SMA springs create an actuation force because of heat generated by the Joule effect when electrical current is conducted through them, while the cooling process may be natural or forced. The heating can be caused by resistance heating due to the electrical current. If the grasper is used for space or maritime application, extremely low temperatures would make the heating process of the springs slower. Therefore, the actuators must be implemented on the grasper in a closed environment with proper insulation. In this case, the lower temperature would be beneficial for the cooling phase. Another scenario is where the grasper would be affected by high environmental temperatures (e.g., desert operation). In this case, the transient temperature of the SMA springs may be reached without electrical current and the springs would be activated. For this type of application, SMA springs with higher transient temperature must be chosen. Therefore, the design framework must take into consideration the environmental impact and also grasp application and purpose.

Other design aspects that should be taken into consideration are corrosion and fatigue among the actuators. SMA materials show superior corrosion resistance [38] and super-long fatigue life [39] over stainless steel. The corrosion resistance of SMA materials gains large interest among biomedical researchers. These characteristics allow the SMA materials to be used in medical implants and invasive surgical instruments [40] and in dental application, but some authors have concern about toxic release of the NiTi material when they come in contact with physiological media [41, 42]. Authors in [43] present the effects of corrosion as comparison between steel springs and SMA spring implemented in dampers where the SMA dampers show reduced sensitivity to corrosion where no overstrength is needed. Researchers also suggest that oxide film is beneficial for the SMAs and prevent corrosion when exposed to increased heat. The authors also suggest that further studies must be conducted to explore the influence of oxide films on the fatigue properties [44]. Also, improving the fatigue resistance of NiTi may often

compromise other mechanical and functional properties [45, 46]. Improved fatigue characteristics could be achieved in a hybrid heterogeneous nanostructure is applied to SMA materials [47]. Researchers in [48] have created a model for estimating the fatigue lifetime. The experimental data had shown that strain rate and mean displacement affect fatigue lifetime. In this research by conducting electricity through the SMA spring they heat up and if the power supply is not deactivated, the temperature may increase dramatically and damage the functionality of the SMA springs. Authors in [49] suggest that the fatigue life of the superelastic materials decreases as the actuation temperature increases. Therefore, an often activation of the SMA springs will definitely lead to functional fatigue overtime. Some of these phenomena were observed in previous research, where after many loading cycles the SMA spring do not return in their original form, rather they show small plastic deformation.

Transformation-induced plasticity (TRIP) plays a crucial role in the fatigue behavior of NiTi shape memory alloys, particularly under cyclic loading, where dislocation slips accumulate and contribute to the process of cracking [50]. Accurately modeling TRIP is essential for predicting the low-cycle fatigue of NiTi alloys, especially in applications where the two-way shape memory effect (TWSME) and large deformations are considered [51]. The TRIP effect is considered while modeling the bridging effects of fibers on crack edges in composite structures with SMA wires, as it significantly influences the boundary between structural continuity and rupture [52].

However, in this work, the focus is not on the material properties, but using the SMAs springs as building blocks into a mechanically intelligent structure for completing a grasper and locomotion task. Several graspers are envisioned to be implemented on top of the transporter. Their multi-locomotion capability for folding would allow space saving during transportation, while crawling and grasping would allow the grasper to leave the vehicle, pass through hardly accessible terrain, grab a certain specimen and return it to the transporter for further exploration. Figure 2a and b shows a CAD model of the vehicle, consisting of the transporter and the dimensions of the transporter, where the two ending positions are shown. Based on the analysis, a prototype of the system has been developed in order to investigate the performance of the structure. Also, it is important to point out that the grasper shown in Fig. 3 represents a case study where the grasper is designed to lift a small flexible object (ball) with relatively small mass. Therefore, detailed analysis must be made in the design stage where the application and the demands should be clearly presented, such as the maximum desired payload capability and object shape and size, and if the target objects are made from stiff or soft material. If the objects are fragile and easily deformed, continuous force distribution must be carefully considered.
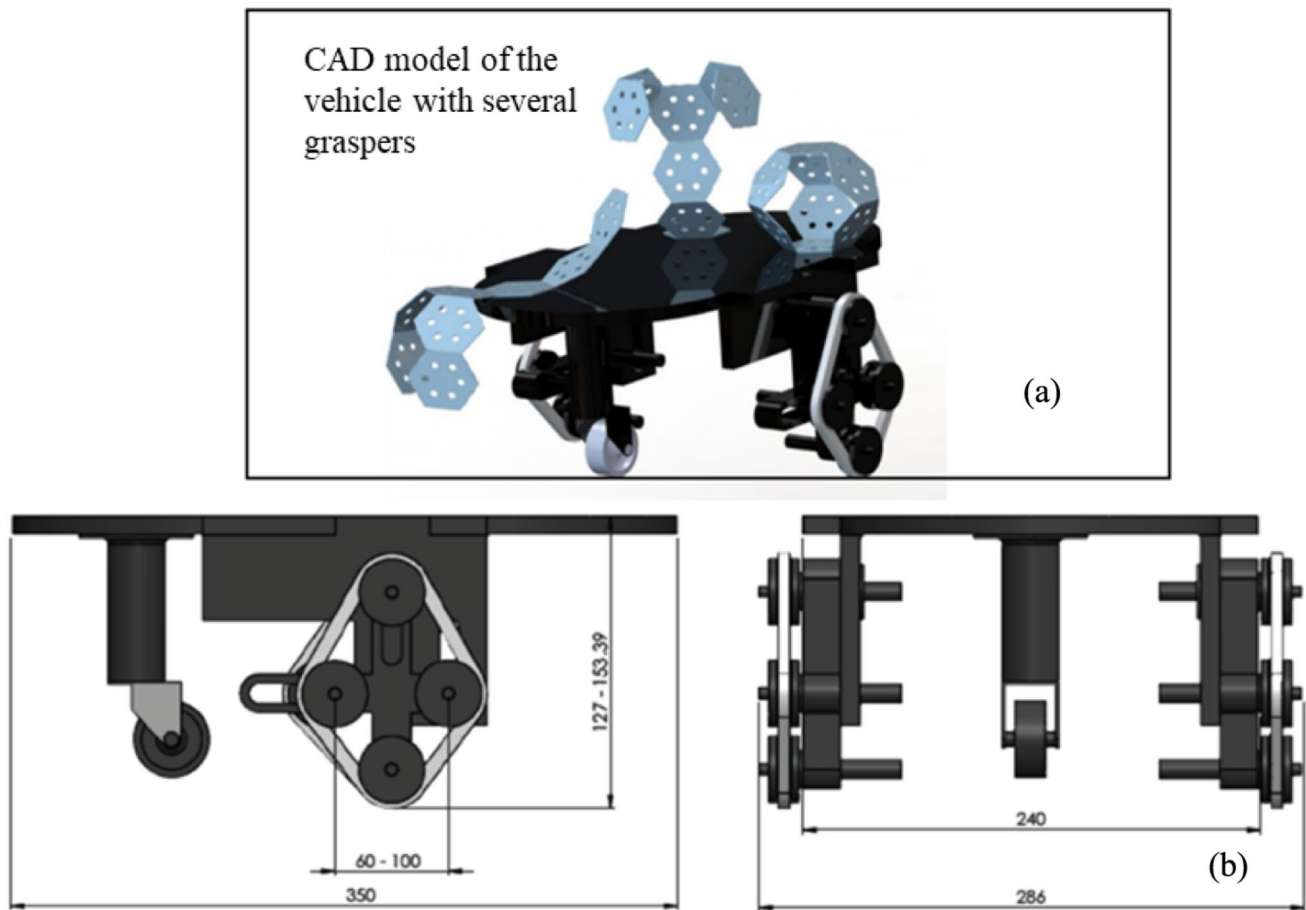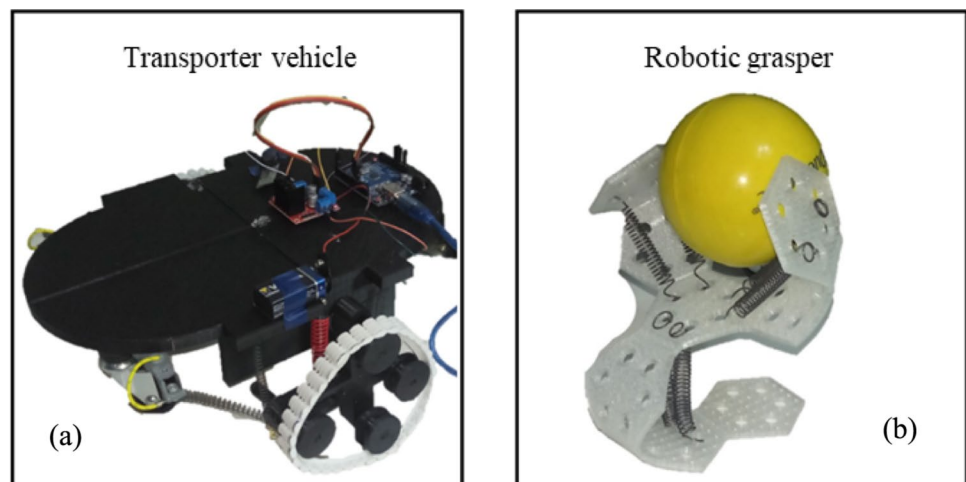
Fig. 2 CAD models of **a** transporter vehicle with several graspers and **b** transporter vehicle dimensions

Fig. 3 Prototype model **a** of the transporter vehicle and **b** the robotic grasper lifting an object

The presented transporter and graspers represent a concept solution with the previously defined dimensions [35].

To enable the mobile grasper to autonomously undock from and dock with the vehicle, various docking mechanisms can be employed for modular robots [53]. One common approach involves the use of magnetic connectors [54], where magnets on the grasper and the vehicle facilitate a secure connection. Alternatively, mechanical connectors [55] such as latches or hooks can be designed for a robust physical connection. These mechanisms often offer a sturdy linkage, but may demand careful engineering to account for alignment and potential wear. Moreover,

electrical connectors can utilize current as a control signal, enabling the grasper to establish a connection with the vehicle through an electronic interface. The mobile grasper's docking mechanism can leverage a novel connector for hybrid chain-lattice type modular robots, featuring an array of electro-permanent magnets embedded in a planar face for precise control over the connection process [56]. Each type of docking mechanism presents its own set of advantages and challenges, and the choice depends on factors such as the application requirements, environmental conditions, and desired autonomy level for the mobile grasper.

The development of an additional variant of the transporter necessitates adjustments to both the grasper's dimensions and the SMA springs. This becomes particularly crucial when designing a scaled transporter, as scaling up or down the transporter requires accommodating graspers of varying sizes. This enhances flexibility during research activities, enabling exploration of confined spaces or transportation of larger objects. In instances where the target specimen is larger than a single grasper can handle, coordination among several graspers becomes essential for lifting the object effectively.

3 Conceptual design of multifunctional structure

Based on the idea of creating bio-inspired multifunctional structure, a single hexagonal cell unit is proposed as shown in Fig. 4a. The form was chosen due to its simplicity and the possibility of attaching several cell units in different directions. Different forms may be applied and studied depending on the application. The dimensions of one unit cell

and the segment (Fig. 4b) formed from three-unit cells are adapted based on different demands and real-life application conditions.

Besides the dimensions of hexagonal cell unit the form of the edges should also be taken into consideration. This was concluded during the experiment phase where the sharp edges of the cell unit provided better gripping of the grasper, but if the ground surface is soft, then the edges may stick in it. Therefore, different shapes of the edges may be introduced. Rounding of the edges reduces the possibility of the grasper getting stuck, but increasing the radius also reduces the friction with the terrain and the crawling functionality. Additionally, engineering the surface of the unit cell should be considered to enhance contact quality. Starting from the unit cell, several bio-inspired design concepts of the proposed multi-functional structure whose idea is to be used as a grasper were analyzed, as shown in Table 1, leading to choosing the most suitable design that has the capability of passing through a rough terrain and obstacles, as it crawls to the desired object, grasps it and crawls back to a transporter or base station. The concept designs are inspired by a caterpillar, scorpion and mantis, and all the models allow the following multi-locomotion movements: crawling, grasping, and folding.

Animals' movement, especially arthropods like caterpillars and scorpions, whose body parts are modular and can be considered as individual segments, represent inspiration for robot's structure. Table 1 shows several design concepts of the grasper. The idea during the decision-making process for a concept that would possess the best features was to implement at least as possible number of cells. Adding one unit cell would imply the addition of an extra Ni–Ti spring. Between the two-unit cells, the SMA springs are positioned, whose actuation can lead to a movement of the
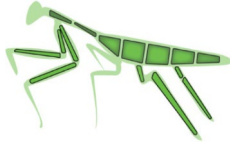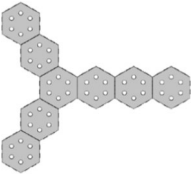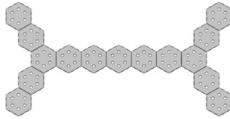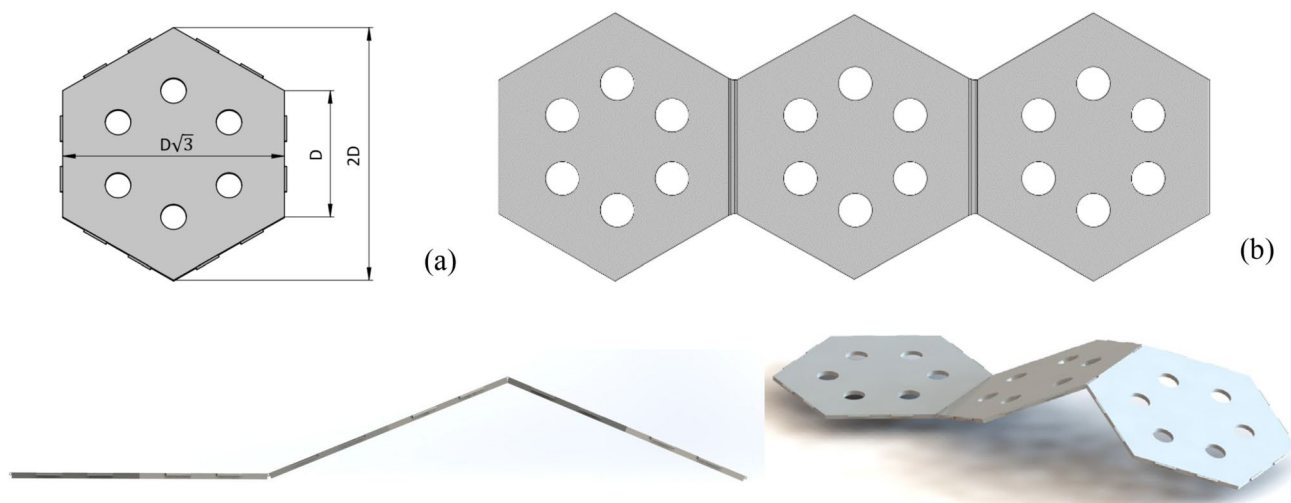

Fig. 4 **a** Form and dimensions of one unit cell **b** One segment is formed from three-unit cells ($D = 25$ mm)

Table 1 Concept design of the robotic grasper

	1st design Caterpillar	2nd design Scorpion	3rd design Mantis
Inspiration			
CAD model			
Number of unit cells	7	8	15

grasper. Therefore, the focus of choosing the final version is on achieving several multi-locomotion movements with optimized mass, number of cells and lowest possible energy consumption. As connection between two cells smaller hinges are applied with the same material characteristics as the cells.

The inspiration for the first design comes from the caterpillar, consisting of 7 unit cells that require a minimum of 6 Ni–Ti springs to operate. It is the simplest model with the smallest number of required Ni–Ti springs, leading to the lowest energy consumption. On the other hand, this concept has a few disadvantages such as the incapability of grasping larger objects. To be able to mimic the crawling process in different directions and achieve the turning process, more SMA springs have to be implemented. The second design is created using 8-unit cells that require a minimum of 7 Ni–Ti springs. Unlike the first version, this concept allows better maneuverability as it forms two segments that can help in performing multifunctionality. This is achieved by adding only one unit cell and one SMA spring. The 3rd version inspired by mantis is created using 15-unit cells and 14 SMA springs. This model allows the best adaptation for any terrain, capability of grasping large objects, but the large number of segments and springs requires more complex control algorithm, precise actuation timing and twice as more energy than the second version.

Considering both the benefits and drawbacks of the suggested designs, the second design has the best performances for the application. The design of grasper has a scorpion tail-like construction that provides modularity by independently actuating the modules. Compared to the other two designs, the chosen design is based on an increased multi-locomotion movement of the grasper compared to the first design and smaller number of SMA springs compared to the third design. Although this design requires more energy

to activate the SMA springs, the position of the segments allow the grasper to grab larger objects and to return them to the vehicle. The two segments help the grasper easier to navigate through rough terrain without increasing the number of SMA springs.

Figure 5 shows several positions of the chosen design of the robotic grasper. The use of bio-inspired structure with integrated SMA springs was used for the development of the grasper. By creating a large-scale deformable body, the grasper could resist unpredicted impacts and reach hard accessible terrains. The actuation of the system is achieved by using SMA springs, which are put through the body on specific spots. The goal in this paper is to analyze the graspers movements, the needed actuation force of the springs in order to choose suitable springs and to optimize the movement trajectory of the grasper and to reduce energy consumption and to achieve faster travel.

The number of cell units for each design is derived for several reasons. To accomplish each movement (grasping, folding, and crawling) a minimum of three unit cells (one segment) is necessary. Therefore, in order to combine two movements simultaneously at least two segments need to be merged. For example, if the grasper is crawling to an object to retrieve it, part of robot must be used for grasping and the other part for crawling. If we analyze the caterpillar design, one segment could be used for grasping and the other segment for crawling. The added "extra" unit cell between these segments is to avoid disturbance between the movements. On the other hand, the same idea is applied in the scorpion design, where one segment is used for crawling, while two "hands" are used for improved grasping. These two "hands" represent two individual segments that use one shared unit cell. This unit cell is also used as an intercell, like the added unit cell in the caterpillar design. To utilize the previous ideas, the
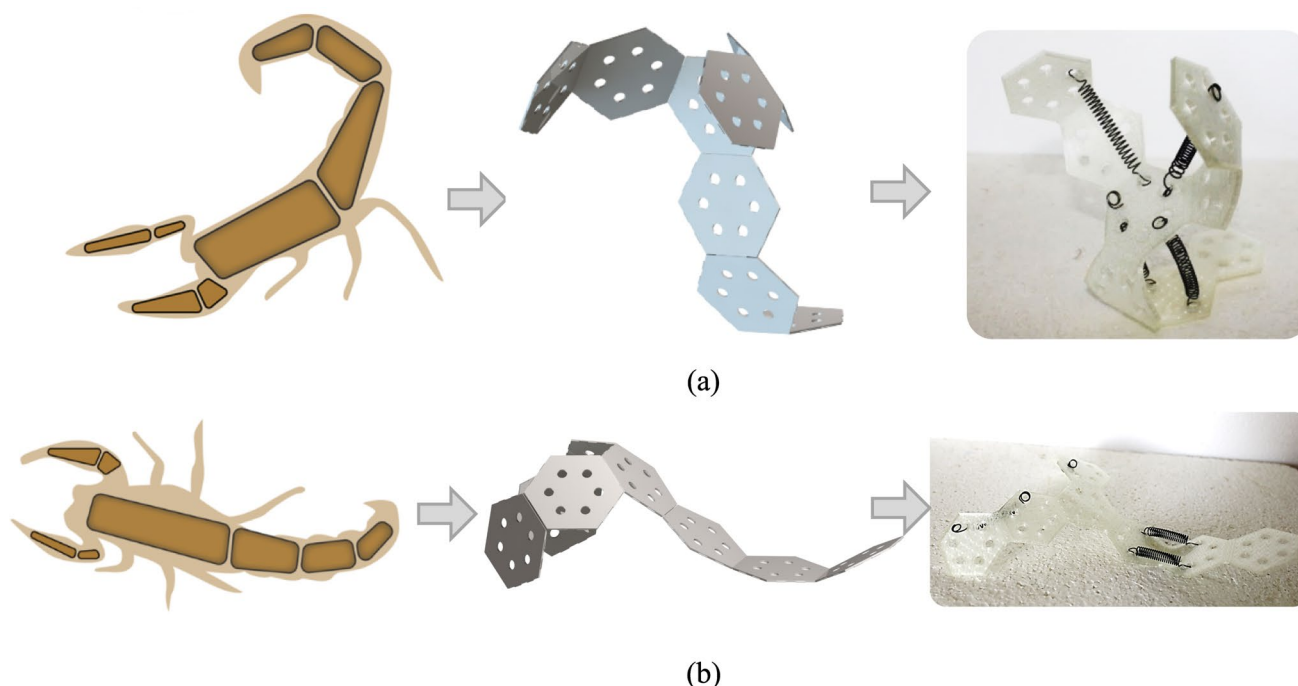
(a)

(b)

Fig. 5 Several positions of the scorpion-inspired robotic grasper: **a** Grasping position and **b** Crawling position

mantis design is created by joining two scorpion designs, in which the central unit cell is shared and belongs to two segments responsible for crawling.

Hence, the overarching concept involves delineating a specific number of segments capable of executing simultaneous multi-locomotion movements. These segments can either share a common unit cell, and if required, an additional unit cell may be introduced to prevent direct interference between the movements. Furthermore, various designs of unit cells can be examined, with the suggested hexagonal configuration appearing most fitting for enabling symmetric segment attachment in different directions.

The design tree can be expanded by adding additional segments to different points of the grasper and would certainly make the grasper more adaptable. However, the goal is to demonstrate the feasibility of achieving diverse movements with a minimal number of segments. This approach aims to significantly decrease the energy required for actuating the grasper, emphasizing efficiency in the overall functionality of the system. If necessary, the proposed design can be scaled up or downsized in order to satisfy different needs or applications.

The main objective of the grasper is retrieving different objects and if the grasper presented in this research paper is consider as a basis. Scaling up the grasper could result in the possibility of retrieving larger specimen which would increase grasper flexibility. Larger graspers are capable of embedding more SMA springs, but also MEMS sensors.

MEMS sensors such as accelerometer or thermal sensors would improve the precision movement of the grasper and support control of the actuators. MEMS thermal sensors could also be used to protect the SMA springs from overheating. Smaller grasper would require a smaller SMA spring that generates smaller forces which would not be able to lift heavy object. But if the design concept and application require downsizing of the grasper, the design framework can take that into consideration. Small MEMS SMA structures are used in biomedical applications [57], intraocular lenses [58] or tactile display [59]. Researchers in [60] suggest the usage of SMA materials in micro-grippers for micro-level object manipulation. From previous mentioned applications, on micro-level and in MEMS structures, the proposed design framework is most suitable for design and creation of MEMS-based micro-graspers/grippers. The application purposes are similar to those presented in this paper, and more detailed observations and analysis will be made in future work.

The grasper is intended to be a freestanding structure while completing a certain task. The attachment only occurs during transport where one or more graspers would be attached to the transporter vehicle. The grasper is attached to the transporter by the central cell unit, and it is in folded position to increase the transport capacity of the vehicle.

Furthermore, the design of the hinges influences the grasper characteristics. The stiffness of the hinges can be modulated for each grasper by changing their parameters

such as form, thickness, and length. In case when a one-way SMA spring is used then the stiffness of the hinges is responsible for returning the grasper into the original position due to elastic energy stored. The moment generated by the hinge stiffness should be able to overcome the SMA spring force at M_f temperature. That means that the stiffness of the hinges would depend on the grasper purpose, dimensions and the SMA actuator forces that would be applied.

In this research, double loop end springs were used where the attachment of SMA springs to the cell unit is conducted using small pins. The holes of the cell unit were used in order to make the connection between the pins and the springs possible. For larger graspers, shafts or bolts can also be used. Either way the connections must be detachable in order to replace or remove the springs in case of service or repair. Also, the position of the SMA spring would directly influence the intensity of the actuator force and moment as presented in the analytical modeling section.

4 Analytical modeling of the movements (grasping, crawling, folding)

To illustrate the segmented approach of the multifunctional grasper, a single segment was modeled while demonstrating its multi-functionality. Analytical modeling is employed to initially determine the optimal number and dimensions of unit cells, as well as the characteristics of SMA springs,

based on the specific application requirements. Therefore, analytical modeling as part of the design framework is responsible for determining the actuator forces of the SMA springs needed. From here, based on the results of the analytical modeling, the SMA springs characteristics and composition can be determined and produced. Another aspect that should be taken into consideration is the ambient temperature of the explored terrain and the transient temperature of the SMA springs. Therefore, by combining the results of the design framework and the demands about grasper's application, appropriate SMA springs can be ordered and produced if the commercially available SMA springs cannot offer the desired characteristics. This study used commercial available SMA springs.

In the following simulations, the desired movements of the grasper have been used as input signals, while as an output data the necessary spring forces were obtained. These data are used to determine the desired SMA characteristics and to implement them in the multi-body analysis.

The movements such as crawling, grasping and folding are shown below. Crawling is a movement that lets the grasper get to the desired location, and while changing the angle of the grasper's cells, other movements such as folding and grasping can be established. These movements lead to multifunctionality of the grasper, allowing successful operating in extreme environments without human intervention. Based on the work in [61], a general modeling approach for tree-like kinematic structures can be used, because of the significant potential as modular robots offer
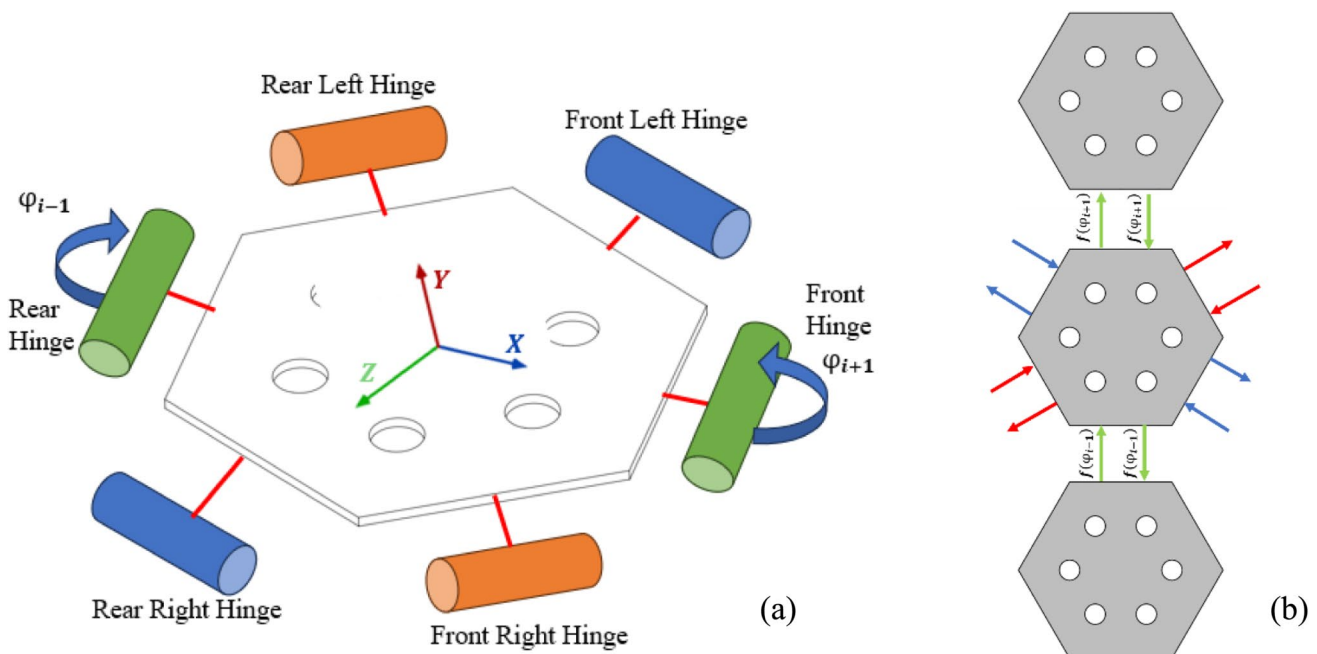

Fig. 6 a Modular kinematic structure shown through a single unit cell b Kinematic tree structure of three unit cells

an extensive design space, making it impractical to create a model for each design individually.

Figure 6a illustrates a modular kinematic structure resembling a tree, shown through a single cell. Each segment allows for the placement of six individual hinges in various directions based on the grasper's design and the number of cells. The unit cell shown in Fig. 5b connects with two other cells using the front and rear hinges. To establish a kinematic model, the relationships, and influences between two cells are showcased through a kinematic modular graph. The relationship between unit cells is directly dependent on the angle between these two cells, denoted as φ_{i+1} and φ_{i-1}. Conversely, in this scenario, the other relations (indicated by red and blue arrows) symbolize potential attachment points and correlations between other cells that can be attached to the central one.

The angle between these two cells is defined by actuator forces generated by the SMA springs and the resistance forces of the material represented by the torsional stiffness coefficient c_t and torsional damping coefficient k_t of the material.

4.1 Analytical modeling–crawling

Schematic representation of grasper locomotion configuration and free-body diagram for crawling mode is shown in Fig. 7. A single segment consisting of three-unit cells is analyzed, same as the presented one in Fig. 4. Segment locomotion configuration presents the proposed positioning of the SMA springs and positioning of the unit cells during the crawling process. In order to conduct analytical modeling the segment locomotion configuration is replaced with free body diagram where the hinges' influence is replaced with stiffness and damping coefficients of the hinges' material

and the interaction between the unit cells and the segment with the ground is replaced by the expected forces.

Equations (1–4) describe the plane movement of the segment. This model has 3 DOF, two translations (x and y) and one rotation φ_i. By defining the desired movement of the entire model and its mass and using this segmented approach, the initial necessary values for the stiffness and damping coefficient can be defined. The actuators forces should be able to overcome the mass of the grasper and the resistance forces in the hinges between the segments. These hinges are represented by the torsional stiffness c_t and damping k_t coefficient of the material. In this paper, SMA springs are chosen to be used as actuators. The equations when modeling this type of movement are shown below:

$$I_z\ddot{\varphi}_i = -c_t\Delta\varphi_{i-1} - k_t\Delta\dot{\varphi}_{i-1} - c_t\Delta\varphi_{i+1} - k_t\Delta\dot{\varphi}_{i+1} - mg\left(\frac{l}{2}\cos\varphi_i - \frac{a}{2}\sin\varphi_i\right)$$
$$+ F_{i-1}\cos\gamma_{i-1}a + F_{i-1}\sin\gamma_{i-1}b - F_{i+1}\cos\gamma_{i+1}a + F_{i+1}\sin\gamma_{i+1}(l-b) \tag{1}$$

$$m\ddot{x}_i = F_{i-1}\cos(\Delta\gamma_1) - F_{\mu(i)} - F_{\mu(i-1)} - F_{\mu(i+1)} - F_{i+1}\cos(\Delta\gamma_2) \tag{2}$$

$$m\ddot{y}_i = F_{i-1}\sin(\Delta\gamma_1) + F_{i+1}\sin(\Delta\gamma_2) - mg \tag{3}$$

$$\Delta\gamma_1 = \gamma_{i-1} - \varphi_i, \Delta\gamma_2 = \gamma_{i+1} + \varphi_i \tag{4}$$

where I_z is the material moment of inertia of the segment, F_{i-1} and F_{i+1} represent SMA spring forces, $F_{\mu(i)}$ represents the friction force between the unit cell and the ground, c_t is the torsional stiffness coefficient of the material, and k_t is the torsional damping coefficient of the material.

Analytical modeling is used to determine the necessary characteristics of the SMA springs in order to achieve desired motion. Thus, the rotation φ_i and translations in the x- and y-directions of one or more segments serve as system inputs. By analyzing the outputs (the forces necessary to
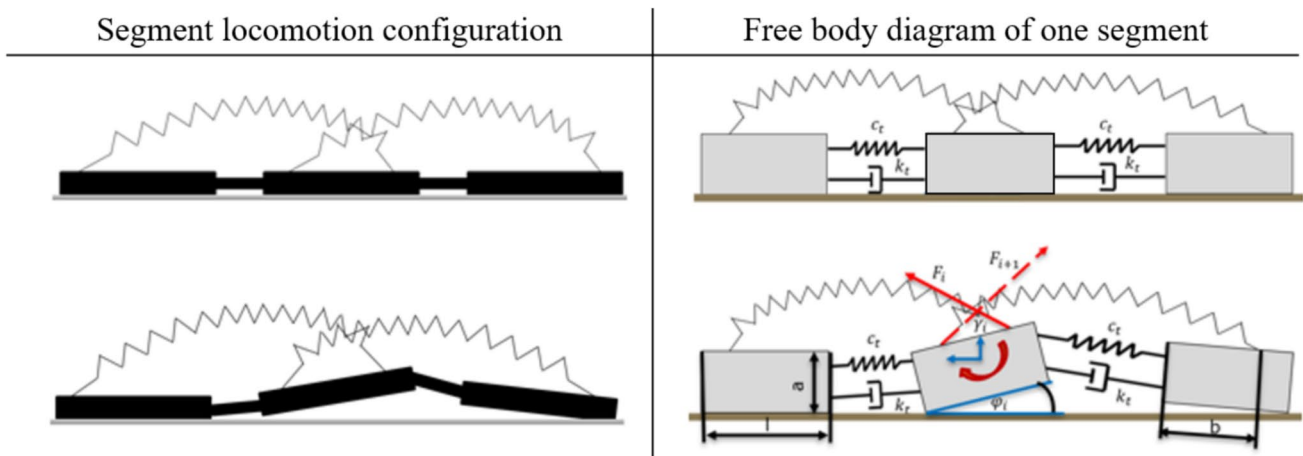

Fig. 7 Segmented approach for analytical analysis of the crawling movement (left: one segment configuration, right: free body diagram of one segment)

achieve the desired motion) an initial indication can be obtained about the SMA springs characteristics.

The proposed analytical model takes in consideration the state of the SMA springs whether they are activated or not. While conducting electricity through them, the stiffness coefficient is changing, and they generate different actuator force. Analyzing the results from the analytical modeling reveals the following conclusion: When the required actuator force is minimal, it indicates that the SMA springs should remain inactive. On the contrary, as the required actuator force increases, activation of the SMA springs becomes necessary. However, it is important to note that the linear characteristics of the hinges, as expressed by their stiffness and damping coefficients, pose a limitation to the analytical model. To address this limitation in future research, a nonlinear characterization of the hinges' bending will be incorporated, as they represent the primary resistive forces.

Figure 8 presents a case study showing the desired movement of the middle cell, which serves as input. Inspired by the caterpillar's motion, each unit executes a sinusoidal movement. The model outputs the minimum required spring forces. This dataset serves as a reference for choosing
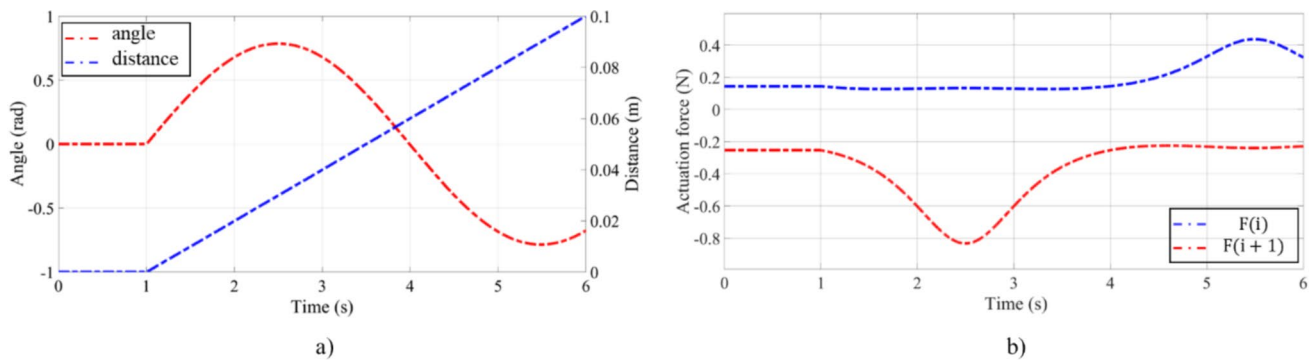

Fig. 8 **a** Input signals to the crawling analytical model and **b** obtained needed force intensity from the model for SMA actuation needed for crawling
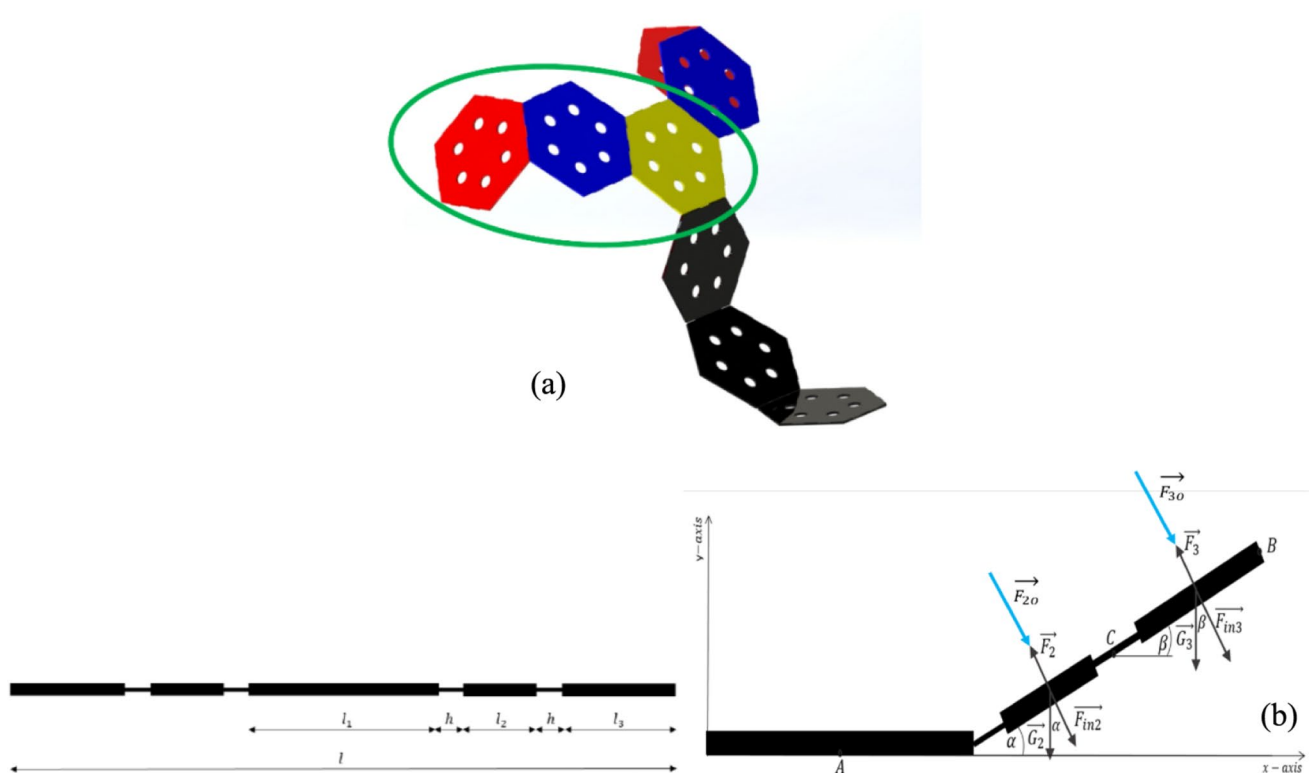

Fig. 9 **a** 3D model of grasper with focus on one hand **b** segmented approach for analytical analysis of grasping and folding movement

SMA springs with specified characteristics tailored to meet the application requirements. In this scenario, the unit cell dimension (*D*) is 25 mm with a thickness of 2.5 mm. The results in Fig. 8 are obtained using the analytical model defined by Eqs. (1–4).

4.2 Analytical modeling–grasping and folding

Figure 9 represents the simplified model of one of the pair segments for grasping and folding. The central unit cell (shown with yellow color) is used as common unit cell for both segments that create the "hands" of the grasper. On the free body diagram, the central unit cell is considered to be fixed.

Just like the analytical model employed for crawling movement, the grasping mechanism utilizes a single segment for determining the motion. After defining the previous described stiffness coefficient and damping coefficient of the hinges, the resistance forces (F_{2o}, F_{3o}) and SMA actuator forces (F_2, F_3) needed to make the grasping movement and to hold the object are added to the model. These forces represent the influence that the grabbed object's has on the grasper. The forces intensity depends on the lifted object's mass, shape and stiffness. In order for the grasper to successfully grasps an object, the SMA actuator forces (F_2, F_3) must overcome the grabbed object's resistance forces, (F_{2o}, F_{3o}) restitution forces of the hinges and unit cells weight (G_2, G_3).

On the other hand, if we define the desired movement, then we can determine the desired grabbing force. According to Fig. 9, Eqs. (5–8) show the mathematical modeling of these movements:

$$\sum F_x = (F_{2i})sin\alpha + (F_{3i})sin(\alpha + \beta) = 0 \tag{5}$$

$$\sum F_y = (F_{2i})cos\alpha - G_2 + (F_{3i})cos(\alpha + \beta) - G_3 = 0 \tag{6}$$

$$\sum M_A = [F_{2i}cos\alpha - G_2] \cdot \left(\frac{l_1}{2} + (h + \frac{l_2}{2})cos\alpha\right) + [F_{3i}cos(\alpha + \beta) - G_3]$$
$$\cdot \left(\frac{l_1}{2} + (h+l_2)cos\alpha + \left(h + \frac{l_3}{2}\right)cos(\alpha + \beta)\right) + F_{2i}\left(h + \frac{l_2}{2}\right)$$
$$sin^2(\alpha) + (F_{3i})sin(\alpha + \beta)\left((h+l_2)sin\alpha + \left(h + \frac{l_3}{2}\right)sin(\alpha + \beta)\right) = 0 \tag{7}$$

$$F_{2i} = F_2 - F_{in2} - F_{2o}, \ F_{3i} = F_3 - F_{in3} - F_{3o} \tag{8}$$

Unlike the previous models, where different variable inputs must be made and they are defined by the current situation, the folding of the grasper is much simpler. The only resistances that should be overcome are the resisting forces of the material and the mass of the grasper. The analytical modeling of the grasper is presented with the previous equations where $F_{2o} = 0, F_{3o} = 0$, but the choice for suitable SMA springs should be made considering the previous movements where the values of the resistance forces and the needed actuator forces are higher. If those movements are reached, it implies that those forces would be enough to achieve the folding too and only the final position of the segments and actuator timing should be defined, depending on the number of segments of the grasper.

Using Eqs. (5–8), another case study of the folding process is presented in Fig. 10 where the trajectories of the grasper's hands are shown. The characteristics and the dimensions of the grasper are the same as in the previous case study. By defining the desired final position of the segments and time needed to achieve that (in this case 3 s), the minimum needed SMA springs' forces are presented. It is interesting to observe that the value for the force F_3 starts from positive value equal to the unit cell weight and then switches sign. This can be explained by the fact that the unit on which the force is applied overlaps more than 90°. This does not mean that the springs expands, but on the contrary,
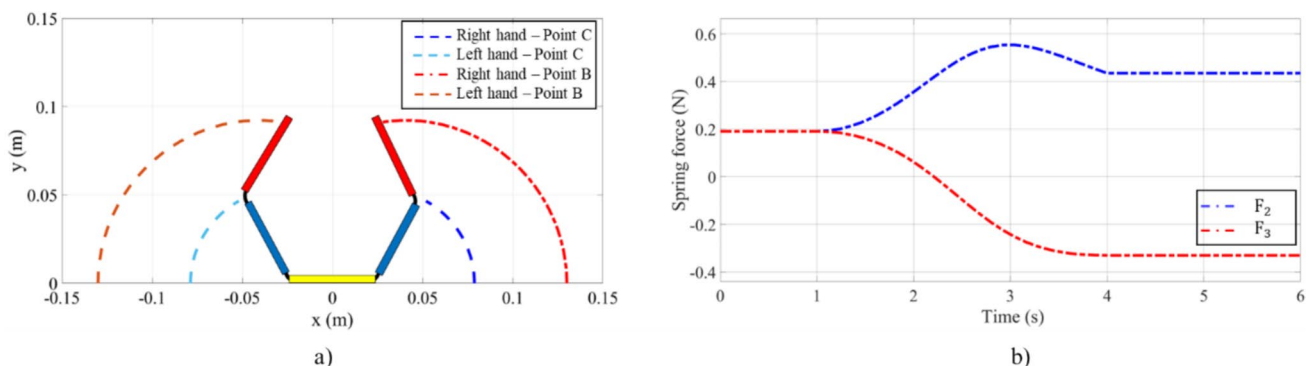

Fig. 10 a Input signals to the grasping/folding analytical model and **b** obtained needed force intensity from the model for SMA actuation needed for folding

the springs remain contracted, with the possibility of generating the desired force. It must be pointed out that these are the necessary minimal forces. If larger force is applied, then the grasper would only fold faster.

Once the transient temperature has been reached, the actuation is almost instantaneous. On the other hand, that means that more than 3 s would be needed for cooling down and returning to original shape. Taking this into account, the SMA springs would be slower than a hydraulic, pneumatic or electric actuator. Adding a cooling system would improve the spring performance, but they would be still slower than the previous mentioned actuators. The SMA springs were chosen as actuators because of their advantage in returning to original shape even after extensive deformation and regaining their performances.

The goal of the presented analytical modeling is to determine the necessary actuator forces thus finding the required SMA springs characteristics. In order to make the analytical modeling more general for different designs and configurations, a more general approach will be introduced in future. We plan to develop solutions for determining the desired movement and configuration of the grasper with the product of exponentials (POE). This method is used for modular robots design described in [61]. Assuming the last unit cell serves as a basis and the "hands" of the grasper act as an end effector, the absolute configuration of the grasper, denoted as $C(\theta)$, can be defined by:

$$C(\theta) = \prod_i e^{\theta_i \xi_i} \tag{9}$$

where θ_i represents the angle rotation of the hinges, while the twist $\xi_i \in \mathrm{SE}(3)$ is defined as $\xi_i = \begin{pmatrix} \vec{\omega} \\ \vec{v} \end{pmatrix}$ for each hinge of the grasper. This could be quite useful because it would not be feasible to come up with analytical model for every design.

Analytical modeling provides the initial values for the actuation forces.

5 Multi-body modeling and optimization of the distributed actuation inputs

In order to explore the system performance, multi-body modeling approach was conducted by using the MSC Adams VIEW software. The multi-body modeling is the next step after the analytical modeling in order to overcome the approximations that were made in the analytical modeling and to test the characteristics of the springs by traveling on different types of terrain. Most importantly, multi-body modeling can be used to optimize the movement of the grasper by correcting the input command to the joint in order to reach the desired location in shorter period of time with similar input signals. By doing this a more sustainable grasper could be achieved. The model was created by using a segmented approach where each segment was connected by revolute joint with 1-DOF (Fig. 11). The material used to define the characteristics of the segments was PLA6 plastic with density of 1200 kg/m3 is the same material that was used for the 3D printing of the model in [26]. Crawling was employed as the movement model in the multi-body system, necessitating the simultaneous activation of actuators. To achieve this specific movement, distinct time dynamic inputs had to be generated for each actuator, ensuring the desired crawling motion is attained. The general idea of the modeling was to stimulate the grasper to achieve one full movement and to be set in a position, ready to make the next step by mimicking the movement of the caterpillar.

The input signals of the actuators were defined as step functions, which determines the angle between two segments. To achieve this angle, the actuators that are implemented in the graspers must be able to achieve this angle and at the same time must be able to generate enough force to make the movement possible. Next step in the ADAMS modeling represents the implementation of springs with stiffness same as the Nitinol springs obtained from the analytical modeling. The input motion between cell units 3 and 4 and spring forces of different springs are presented in Fig. 12.

These springs represent the actuators and at the same time represent the sensors that were implemented into the model to measure the necessary force (in this case—spring force) needed to generate the desired movement.

The results of the needed forces for several springs are represented in Fig. 12. In the cases the characteristics of the springs are obtained from testing of real SMA springs. Their stiffness coefficient is 153 N/m in heated state, while on ambient temperatures is 59.5 N/m. For the simulation, it is assumed that the springs are in heated state which would allow lower response time for their activation. Also, it is important to state that between two unit cells a pair of two springs is positioned. For example, between cell units 3 and 4, spring 5 and spring 6 are positioned. This means that the total force needed to lift the two cell units would be the sum of the forces spring 5 and 6. Usually, the force in a pair of springs is equal so the needed force is double the value of one spring force.

The maximum needed force of around 0.4 N corresponds with the SMA springs analyzed in [26], confirming that these springs can be used as actuators in the proposed model. Also, it is important to mention that in order the grasper to work properly, two springs capable of generating a force of 0.4 N must be applied, or one stiffener spring capable of generation at least 0.8 N. This value also corresponds with the maximum spring force value obtained from the
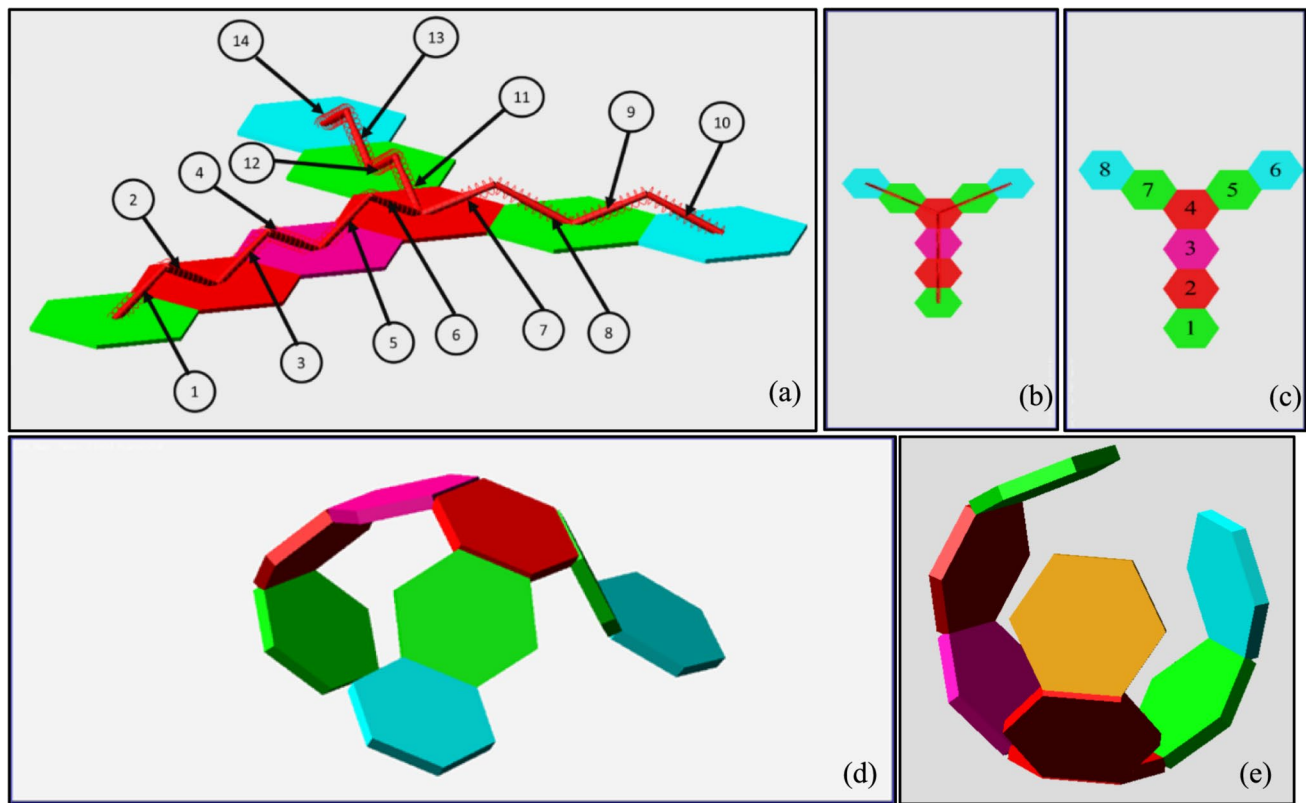
Fig. 11 ADAMS model of the Grasper in several positions: **a** Location and index number of each spring; **b** Grasper in flat position—springs are not activated; **c** Location and index number of each cell unit; **d** Crawling—all springs are activated and stimulated at different timing and input signals; **e** Folding—all springs are activated and stimulated at simultaneously

Fig. 12 Measured spring forces intensity between two segments from the multi-body simulation
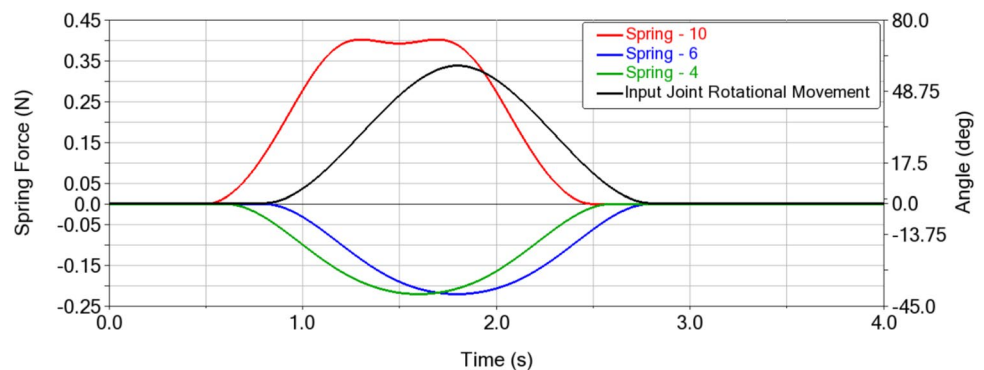
analytical modeling. The proposed model can be used for analyzing different variants of the grasper such as scaled or downsized grasper, actuators with different characteristics, even different cell shapes which would lead to different forms of the grasper. By doing these kinds of modifications of the model, many cases can be analyzed. If several types are satisfactory, then several of them can be used in coordination between themselves and the transporters which would result in increased flexibility of the system.

Different external forces that would represent different obstacles or object may be implemented in order to test the response of the model and their influence. Because the final goal of the concept is space exploration or remote locations, in order to retrieve some desired specimens many obstacles cannot be precisely estimated, and also many unpredicted problems may occur during the space operations. Therefore, the multi-body modeling approach may help in testing these unpredicted forces and obstacles as random external disturbances and further optimize the grasper models.

In order to improve the velocity of the grasper and reduce energy consumption of the actuators, optimization was applied. Optimization process was applied using the ADAMS's software by applying generalized reduced gradient (GRG) which is an extension of the reduced gradient method able to accommodate nonlinear inequality constraints [62]. The optimization led to improved activation timing of the actuators.

The goal of this research was to optimize the value of the angles between the segments in order to achieve maximum
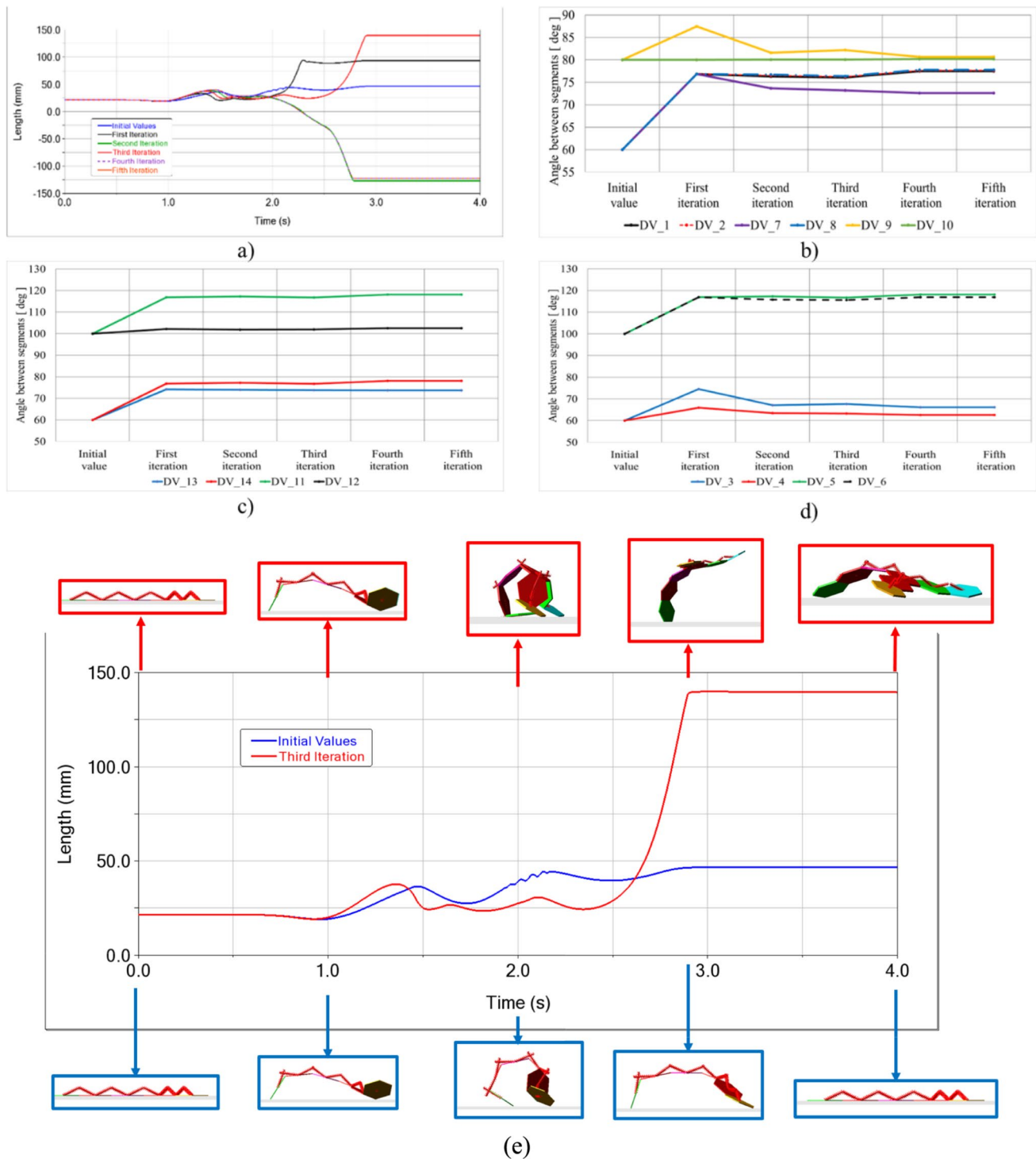

Fig. 13 Multi-body optimization process: **a** Distance traveled by the grasper in different optimization iterations and variations; **b–d** Initial and final values of the variables after the optimization process, **e** comparison between the movements of the initial and optimized model

travel distance of the robot. In the optimization process, the angles were set as variables in wider range as they are important to define the output commands of the actuators, while the timing of their activation remained the same. As shown in Fig. 13a, only a few iterations gave negative results and forced the grasper to travel in different direction. The third iteration showed the best results. Also, it can be observed that the optimized model can cover 4 times more distance in only one movement. Figure 13b–d also shows the maximum value of the angles during each iteration and for each variable. The results showed small differences between the initial and final values of the variables, showing improved results by just having small corrections in actuators input signals. Figure 13e shows the comparison between the initial grasper movement (bottom) and the optimized one (top). Besides the larger trajectory, the position of the graspers in each second of the simulation. The top figures represent the optimized grasper, while the lower figures show the initial movement of the grasper.

The optimization led to great improvement, raising the travel distance by more than 400%. This shows that with the identical timing of the actuators and by defining the right output signal and commands, an optimal movement of the grasper can be achieved which would result in faster travel velocity and less energy consumption. All of this proves that the multi-body is capable of modification based on the application and the demands for the grasper, as well as in power and actuation modeling and optimization, resulting in more sustainable robots.

The optimization allows improved design and grasper actuation, which is presented in the results and confirmed in the experiments. Our future research will be focused more on the optimization algorithms and their influence on further improvement of the design framework. Optimization could also be done as co-simulation between ADAMS and MATLAB/Simulink, thus enhancing the advantages of both multi-body and analytical modeling.

Table 2 SMA springs characteristics

Material	NiTiCu
Length when heated:	20 mm
Maximum deformation	150 mm
Transition temperature	65 °C
Stiffness coefficient when heated:	153 N/m
Stiffness coefficient in ambient temperature:	59.5 N/m

6 Experimental setup and results

In order to test the proposed design framework, several experiments were conducted. A 3D-printed grasper model was created using PLA6 material, and several SMA springs (Ni–Ti) were implemented as actuators. The characteristics of the springs are presented in Table 2.

The SMA springs are made from Ni–Ti–Cu alloy and can be deformed up to 150 mm in martensite phase, while when heated in austenite phase they return to their original length of 20 mm. The starting temperature of the austenite transformation is $A_s = 50°$ and the process is complete at temperature of $A_f = 65°$. During the cooling process the starting martensite temperature is $M_s = 40°$ and is completed at temperature $M_f = 32°$.

The experiment used an SMA spring connected to a 12 V power supply, a digital multimeter for temperature measurement, and a ruler for length measurement. A temperature sensor was attached to the spring. To determine austenite transformation temperatures, the spring was stretched to 100 mm and then heated. The austenite start temperature (A_s) was identified when the spring began contracting, generating force but not fully returning to its original 20 mm length. The transformation completed at A_f when the spring fully retracted, and power was then turned off to prevent overheating.

For martensite transformation, the spring was first heated to A_f, then force with small intensity was applied. In the austenite state, the spring resisted elongation, but as cooling began, deformation was first observed at 40 °C (M_s). The transformation concluded at $M_f = 32$ °C when the spring suddenly gained significant strain.

Stiffness tests showed a coefficient of 153 N/m in the heated state and 59.5 N/m in the martensite state. The spring was mounted on a vertical stand with a ruler for deformation measurement. Weights were added incrementally in martensite and austenite states, and stiffness was calculated using Hooke's law. The austenite test included heating above A_f while maintaining temperature via electrical current.

The actuation of the springs is executed by applying electricity through them. By using their resistive characteristics, they are heated to temperature of 70°, above defined A_f temperature. When the A_f temperature is reached, the springs contract and pull the grasper's unit cells toward each other. For this actuation a power supply of $V = 12V$ is used, capable of withstanding current of 10 A. As the electricity runs through the SMA springs the current reaches value of $I = 6.67A$ and the SMA springs are heated up to 70°. At this moment, the power supply is stopped in order to prevent overheating and damaging of the springs. To heat the SMA helical springs Joule

effect is utilized and from the measured parameters it can be concluded that the SMA springs are actuated by power supply of approximately $P = VI = 12 \cdot 6.67 \approx 80W$ (Eq. (10)).

$$P = VI \qquad (10)$$

Resistance measurements showed 1.3 Ω in the martensite phase at 20 °C and 1.799 Ω at 70 °C in the austenite state, measured with a digital multimeter. Due to the fact that the SMA spring acts like a resistor, an approximation is made that the resistance changes linearly while heating using Eq. (11):

$$R = R_0(1 + \alpha \Delta T) \qquad (11)$$

where α represents the temperature coefficient and ΔT the temperature difference while heating.

By replacing the measured values in the equation the temperature coefficient for this SMA springs is calculated to be $\alpha = 7.68 \cdot 10^{-3} C^{-1}$.

From the presented results and by combining Eqs. (10) and (11), a relationship between the power supply and the temperature rise could be derived in Eq. (12).

$$\Delta T = \frac{\left(\frac{V^2}{PR_0} - 1\right)}{\alpha} \qquad (12)$$

During experimental work and after prolonged use of SMA springs fatigue started to occur, some of the springs even had 50% strain that could not be recovered and when heated up they return to length of 30 mm instead of 20 mm. The springs are still functionable, but their shape memory form is changed. The attachment of the springs to the grasper is shown in Fig. 14a. During the research and experimental phase, power supply with high current capacity was used.

All connections from the SMA springs and wires were combined in one power supply, but they are stimulated independently. In future research a more powerful power supply and controller would be used where the SMA springs will be actuated simultaneously. Because of the high
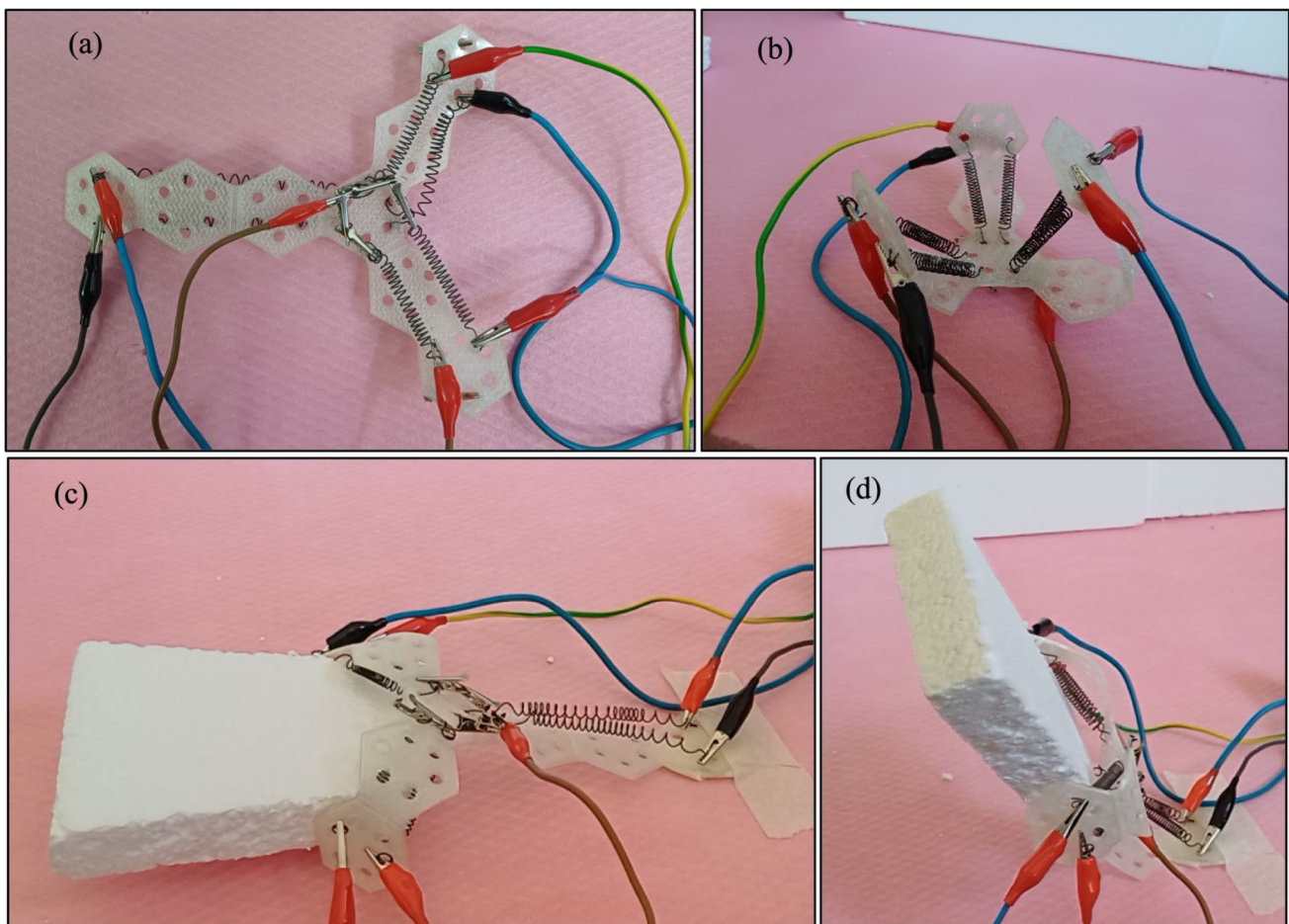

Fig. 14 Experiments of folding and grasping process. **a** 3D-printed grasper with the attached SMA springs; **b** Folding of the grasper; **c, d** Grasping of an object

resistance of the SMA springs, the power supply should be capable of generating stronger current. In this case study, we cannot use only one SMA spring for the entire structure because it can only achieve folding. But, if stiffer SMA springs are used, then their number can be reduced to one SMA spring per segment. At the end of the actuation the power supply is disconnected in order to allow the springs to cool down and return the grasper in the original position or to rotate the cell unit back with the help of the hinge stiffness. Prolonged actuation may lead to excessive heating and losing the SMAs characteristics.

In this case study, six SMA springs were used to actuate the grasper in order to achieve each of the multi-locomotion movements. Two springs are responsible for actuating one segment of the grasper. Folding of the grasper is presented in Fig. 14b. The heated springs generated force is around 0.87 N each, measured indirectly based on the displacement of the springs. These forces are larger than the minimum needed of 0.4 N. The only negative side of the folding process is the requirement of constant power supply to the grasper that could lead to continuous battery drain.

Grasping of an object was also successfully achieved by grabbing larger object. The grasping process is presented in Fig. 14c and d. Similar to the folding experiment, the actuating forces were measured indirectly and lifting of the object was achieved with generated force of 0.87 N per spring, higher than the minimum required. This can be explained due to the fast responsiveness of the springs when they reach transient temperature and in that moment the generated force grows several times more than in ambient temperature.

The crawling movement as the most complex of all presented movements and the one that we focused on during the multi-body analysis is presented in Fig. 15a. The actuation signals applied to the grasper were determined using the optimized multi-body model. The experiment highlighted the potential of both the proposed grasper design and our comprehensive design framework. Remarkably, the grasper managed to cross a relatively significant distance relative to its size. However, as previously mentioned, deviations between the results of the analytical and multi-body modeling are anticipated due to the downscaled model and reduced number of springs.

After conducting one iteration of crawling the covered distance of the grasper is 98 mm. Compared to results of the multi-body analysis there, the covered distance around 118 mm. The error between the multi-body analysis and the real grasper is 20 mm which is in the desired limits. Therefore, we can conclude that the results confirm our proposed concept and design framework. The error is a result due to the limitations of the one-way shape memory alloy. For example, if we observe the optimized multi-body model in Fig. 13, near the third second of the simulation the grasper makes a leap that covers more distance than in the previous simulation time. This leap in the simulation is achieved by straightening the unit cells 2, 3 and 4. While this process in the simulation is achieved by changing of the input hinge angle continuously and by an input command, in the experiment that was achieved by the elasticity of the grasper and the hinges' stiffness. This process lasted longer due to the time interval needed to cool down the SMA springs and with that to reduce their stiffness. For future research two-way springs will be implemented, in order to achieve actuation force in the opposite direction that would be capable actuate the grasper faster and perform a "leap" similar to the one presented in the simulation.

The entire experiment of crawling compared to the multi-body simulation is presented in Fig. 16. The results and the experiments had shown the potential of the concept and the design framework. The small difference of the results also contributes in the proposed concept of the design
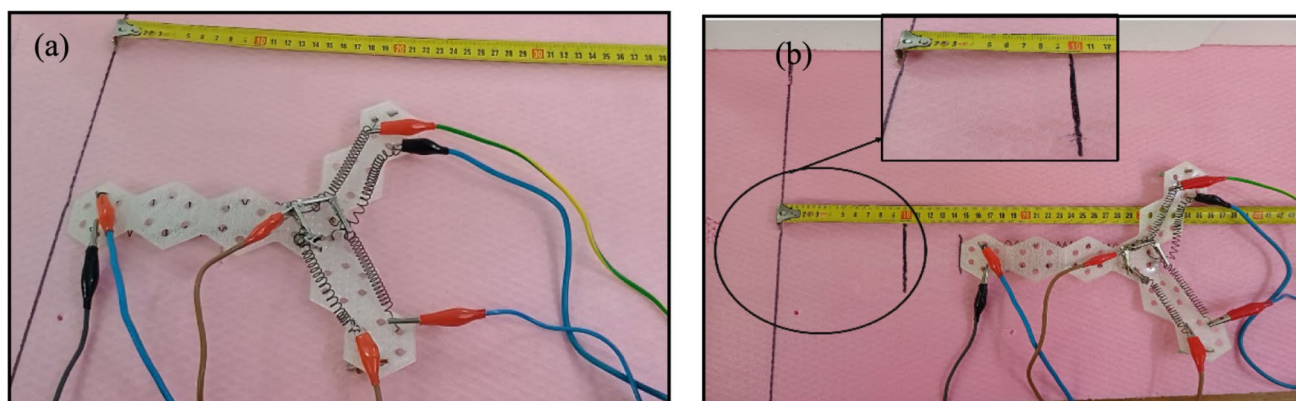

Fig. 15 Experiments of the grasper crawling movements: **a** Starting position of the grasper before crawling; **b** Covered distance of the grasper during one iteration of crawling
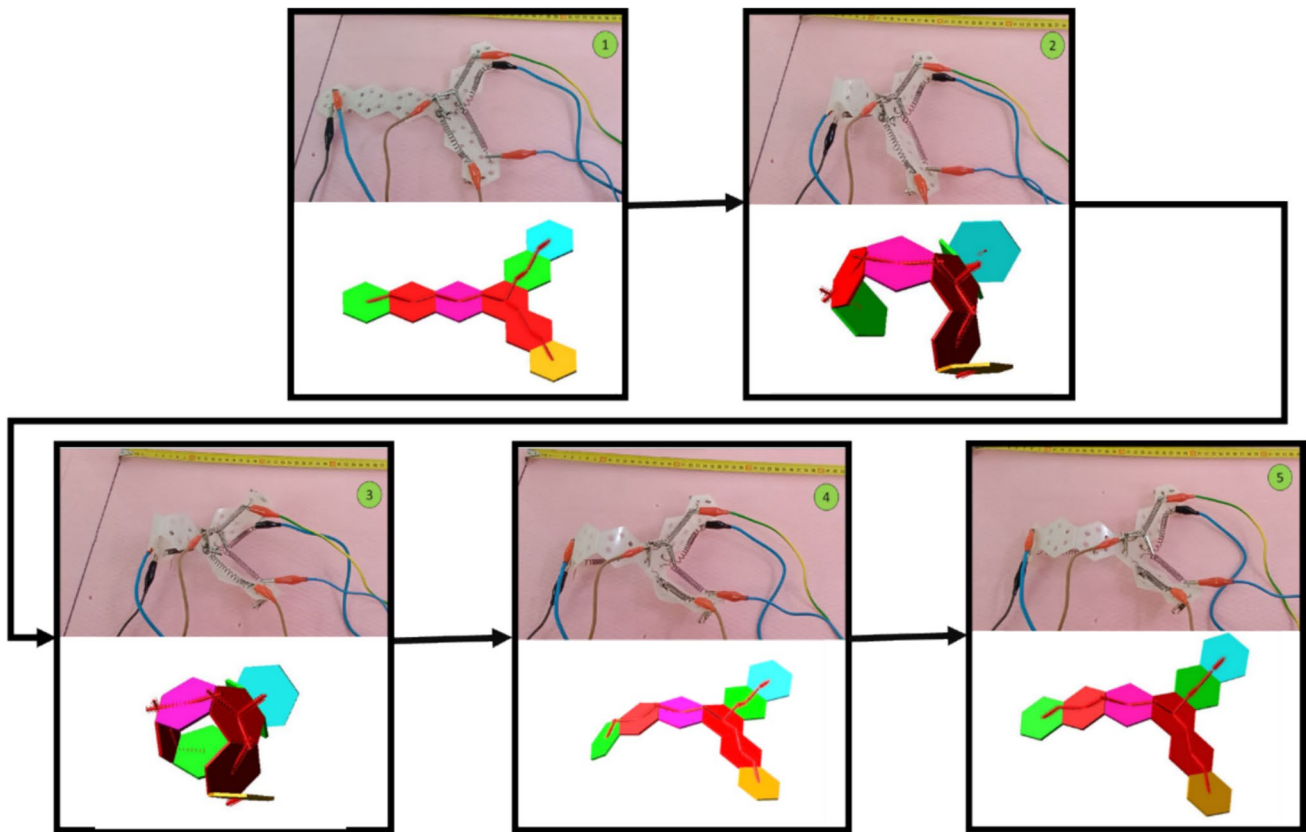
Fig. 16 Comparison of the crawling movement between the optimized grasper in multi-body simulation and the prototype. The movements are presented in 5 different steps

framework, where any deviation in the results in the experiments would result in another iteration in the design process, or in the multi-body analysis. To improve the design, rounding of the edges of the unit cells or at least some of them could be included. This was observed during the experiment where sharper edges of the unit cells result in better traction and friction during the crawling movement, but during experimentation it led to grasper getting stuck on the surface from time to time. This was especially the case of the sharp edges of the grasper's "hands."

Another improvement in the design could be achieved by adding additional hooks to the grasper's "hands" in order to achieve better gripping. On the other hand, in our future research several improvements in the actuation will be made such as implementing two-way SMA springs, adding cooling system for the SMA springs for achieving faster response time and implementation of improved controller. The experiments had also shown the need for controller that is capable of withstanding higher current due to the resistance of the SMA springs.

7 Conclusion and future work

In summary, this work presents a design framework for mechanically intelligent structures, demonstrating through the design of bio-inspired robotic grasper. This grasper design has several advantages over conventional designs: flat structure allows for easy manufacturability, but also effective and precise movements based on various stimuli; the combination of the grasper's body and smart-material actuation provides high flexibility and complexity of motion; and scalability of the grasper can be directly linked to its environmental and operational conditions. Employing a segmented approach and determining initial values for the actuators can enhance decision-making in early stage when implementing SMA springs in the design. Creating a multi-body model of the grasper with the actual number of segments facilitates more accurate performance understanding. Optimization of actuation timing and segment angles, along with suitable actuators, has resulted in a faster and more energy-efficient grasper, particularly crucial in rough terrains and extreme conditions where battery life is vital.

The conducted optimization of the actuator timing increases the traveled distance of the grasper from 25 to 118 mm in one iteration. This concludes that besides the SMA characteristics, the actuation process and timing are equally important. The experiments conducted on the 3D-printed grasper confirm the potential of the design framework as the prototypes demonstrate crawling movement similar to the multi-body model with deviation in the travel distance by 17%.

Potential upgrades to the physical model include implementing two-way SMA springs and a cooling system to expedite spring actuation. The use of two-way springs would require less stiffer grasper; specifically, less effort would be required in determining the rightful hinge stiffness. In this case, the springs themselves will force the grasper to return to its original state while cooling. Also, two operating temperatures must be determined and if necessary different spring stiffness at the different temperature. The addition of two-way spring could remove the need of a cooling system if the difference between the operating temperatures is small. This is because the spring would start to generate extension force quickly after being heat up. If the difference between the operating temperatures is larger, then a cooling system will definitely help to achieve faster activation of the springs. The suggested improvements for the grasper design will be implemented and tested in future.

To enable implementation of a docking station to our concept, we foresee magnetic connectors. This can be achieved by placing electromagnet in one or more unit cells. The concept is chosen because it can be activated or deactivated by grasper's embedded controller. The proposed design framework serves as a valuable tool for designers, engineers, and roboticists to leverage smart materials for actuation, paving the way for a new generation of remote robots capable of operating in real-world conditions. Furthermore, this framework can be expanded to incorporate multiple smart materials into the mechanical intelligence of future robots.

Overall, the design framework concept holds promise for streamlining the actuator decision-making process, optimizing actuators' inputs through multi-body modeling, and reducing the need for trial and error in the prototyping phase. This would ultimately lead to faster robotic design processes and more sustainable robotic graspers.

Data availability No datasets were generated or analyzed during the current study.

Declarations

Conflict of interest The co-author Jovana Jovanova is serving as a associate editor for the Journal of the Brazilian Society of Mechanical Sciences and Engineering.

References

1. Chen R, Yuan Z, Guo J, Bai L, Zhu X, Liu F et al (2021) Legless soft robots capable of rapid, continuous, and steered jumping. Nat Commun 12(1):7028. https://doi.org/10.1038/s41467-021-27265-w

2. Yu M, Yang W, Yu Y, Cheng X, Jiao Z (2020) A crawling soft robot driven by pneumatic foldable actuators based on Miura-ori. In: Actuators, vol 9. No. 2, MDPI, p 26 https://doi.org/10.3390/act9020026

3. Mazzolai B, Mondini A, Tramacere F, Riccomi G, Sadeghi A, Giordano G et al (2019) Octopus-Inspired soft arm with suction cups for enhanced grasping tasks in confined environments. Adv Intell Syst 1(6):1900041. https://doi.org/10.1002/aisy.201900041

4. Chen Y, Zhao H, Mao J, Chirarattananon P, Helbling EF, Hyun NSP et al (2019) Controlled flight of a microrobot powered by soft artificial muscles. Nature 575(7782):324–329. https://doi.org/10.1038/s41586-019-1737-7

5. Sadeghi A, Del Dottore E, Mondini A, Mazzolai B (2020) Passive morphological adaptation for obstacle avoidance in a self-growing robot produced by additive manufacturing. Soft Rob 7(1):85–94. https://doi.org/10.1089/soro.2019.0025

6. Fukuda T, Hasegawa Y, Sekiyama K, Aoyama T (2012) Multi-locomotion robotic systems: new concepts of bio-inspired robotics, vol 81. Springer, Berlin

7. Low KH, Hu T, Mohammed S, Tangorra J, Kovac M (2015) Perspectives on biologically inspired hybrid and multi-modal locomotion. Bioinspir Biomim 10(2):020301. https://doi.org/10.1088/1748-3190/10/2/020301

8. Lu H, Zhang M, Yang Y, Huang Q, Fukuda T, Wang Z, Shen Y (2018) A bioinspired multilegged soft millirobot that functions in both dry and wet conditions. Nat Commun 9(1):3944. https://doi.org/10.1038/s41467-018-06491-9

9. Cianchetti M, Calisti M, Margheri L, Kuba M, Laschi C (2015) Bioinspired locomotion and grasping in water: the soft eight-arm OCTOPUS robot. Bioinspir Biomim 10(3):035003. https://doi.org/10.1088/1748-3190/10/3/035003

10. Peraza Hernandez EA, Hartl DJ, Malak RJ Jr, Akleman E, Gonen O, Kung HW (2016) Design tools for patterned self-folding reconfigurable structures based on programmable active laminates. J Mech Robot 8(3):031015. https://doi.org/10.1115/1.4031955

11. Mao S, Dong E, Xu, M, Jin H, Li F, Yang J (2013) Design and development of starfish-like robot: Soft bionic platform with multi-motion using SMA actuators. In: 2013 IEEE international conference on robotics and biomimetics (ROBIO), IEEE, pp 91–96 https://doi.org/10.1109/ROBIO.2013.6739441

12. Jovanova J, Domazetovska S, Frecker M (2018) Modeling of the interface of functionally graded superelastic zones in compliant deployable structures. In: Smart materials, adaptive structures and

intelligent systems, vol 51951. American Society of Mechanical Engineers. p V002T06A013 https://doi.org/10.1115/SMASIS2018-8176

13. Jovanova J, Domazetovska S, Changoski V (2019) Smart material actuation of multi-locomotion robot. In: Smart materials, adaptive structures and intelligent systems, vol 59131. American Society of Mechanical Engineers, p V001T06A011 https://doi.org/10.1115/SMASIS2019-5675

14. Delda RNM, Basuel RB, Hacla RP, Martinez DWC, Cabibihan JJ, Dizon JRC (2021) 3D printing polymeric materials for robots with embedded systems. Technologies 9(4):82. https://doi.org/10.3390/technologies9040082

15. Yoshida H, Igarashi T, Obuchi Y, Takami Y, Sato J, Araki M et al (2015) Architecture-scale human-assisted additive manufacturing. ACM Trans Gr (TOG) 34(4):1–8. https://doi.org/10.1145/2766951

16. Jovanova J, Domazetovska S, Changoski V (2019) Modeling and prototyping of self-folding origami structure. In: Smart materials, adaptive structures and intelligent systems, vol 59131. American Society of Mechanical Engineers. p V001T06A012 https://doi.org/10.1115/SMASIS2019-5676

17. Var SC, Jovanova J (2023) Design of a soft underwater gripper with SMA actuation. In: Smart materials, adaptive structures and intelligent systems, vol 87523. American Society of Mechanical Engineers, p V001T06A013 https://doi.org/10.1115/SMASIS2023-111702

18. Xiong Y, Ge Y, Grimstad L, From PJ (2020) An autonomous strawberry-harvesting robot: design, development, integration, and field evaluation. J Field Robot 37(2):202–224. https://doi.org/10.1002/rob.21889

19. Bouman A, Ginting M F, Alatur N, Palieri M, Fan D D, Touma T et al (2020) Autonomous spot: long-range autonomous exploration of extreme environments with legged locomotion. In: 2020 IEEE/RSJ international conference on intelligent robots and systems (IROS), IEEE, pp 2518–2525 https://doi.org/10.1109/IROS45743.2020.9341361

20. Dang T, Mascarich F, Khattak S, Papachristos C, Alexis K (2019) Graph-based path planning for autonomous robotic exploration in subterranean environments. In: 2019 IEEE/RSJ international conference on intelligent robots and systems (IROS), IEEE, pp 3105–3112 https://doi.org/10.1109/IROS40897.2019.8968151

21. Zhang C, Zhu P, Lin Y, Jiao Z, Zou J (2020) Modular soft robotics: Modular units, connection mechanisms, and applications. Adv Intell Syst 2(6):1900166. https://doi.org/10.1002/aisy.201900166

22. Liu C, Lin Q, Kim H, Yim M (2023) SMORES-EP, a modular robot with parallel self-assembly. Auton Robot 47(2):211–228. https://doi.org/10.1007/s10514-022-10078-1

23. Li S, Awale SA, Bacher KE, Buchner TJ, Della Santina C, Wood RJ, Rus D (2022) Scaling up soft robotics: a meter-scale, modular, and reconfigurable soft robotic system. Soft Robot 9(2):324–336. https://doi.org/10.1089/soro.2020.0123

24. Whitman J, Bhirangi R, Travers M, Choset H (2020) Modular robot design synthesis with deep reinforcement learning. In: Proceedings of the AAAI conference on artificial intelligence, vol 34. No. 06, pp 10418–10425 https://doi.org/10.1609/aaai.v34i06.6611

25. Campos de Almeida T, Marri S, Kress-Gazit H (2020) Automated synthesis of modular manipulators' structure and control for continuous tasks around obstacles. Robotics: science and systems 2020

26. Cho D, Park J, Kim J (2021) Automatic actuation of the anti-freezing system using SMA coil springs. Metals 11(9):1424. https://doi.org/10.3390/met11091424

27. Rahgozar N, Shahria AM (2023) A novel hybrid self-centering piston-based bracing fitted with SMA bars and friction springs: analytical study and seismic simulation. J Struct

Eng 149(6):04023055. https://doi.org/10.1061/JSENDH.STENG-11938

28. Lv H, Huang B (2024) Vibration reduction performance of a new tuned mass damper with pre-strained superelastic SMA helical springs. Int J Struct Stab Dyn 24(05):2450047. https://doi.org/10.1142/S0219455424500470

29. Sun H (2022) Vibration analysis and control of the suspension system of the drum washing machine by applying SMA. In: Journal of physics: conference series, vol 2200. No. 1, IOP Publishing, p 012009 https://doi.org/10.1088/1742-6596/2200/1/012009

30. Huang Y, Fan Q, Zhang H, Shao L, Shi Y (2024) Optimization of dynamic characteristics of rubber-based SMA composite dampers using multi-body dynamics and response surface methodology. Appl Sci 14(21):10063. https://doi.org/10.3390/app142110063

31. Liu T, Zhu L, Luo J, Dong YR, Li Z (2023) Experimental, mathematical model, and simulation of a dual-system self-centering energy dissipative brace equipped with SMA and variable friction device. J Constr Steel Res 211:108219. https://doi.org/10.1016/j.jcsr.2023.108219

32. Jin H, Ouyang Y, Chen H, Kong J, Li W, Zhang S (2021) Modeling and motion control of a soft SMA planar actuator. IEEE/ASME Trans Mechatron 27(2):916–927. https://doi.org/10.1109/tmech.2021.3074971

33. Ali HF, Kim Y (2021) Design of a 2 DOF shape memory alloy actuator using SMA springs. In: Information storage and processing systems, vol 84799. American Society of Mechanical Engineers. p V001T09A006 https://doi.org/10.1115/ISPS2021-65257

34. Ali HF, Khan AM, Baek H, Shin B, Kim Y (2021) Modeling and control of a finger-like mechanism using bending shape memory alloys. Microsyst Technol 27:2481–2492. https://doi.org/10.1007/s00542-020-05166-0

35. Changoski V, Domazetovska S, Anachkova M, Jovanova J (2020) Autonomous multifunctional vehicle with integrated bio-inspired SMA actuated grasper. In: Smart materials, adaptive structures and intelligent systems, vol 84027. American Society of Mechanical Engineers. p V001T06A006 https://doi.org/10.1115/SMASIS2020-2343

36. Nemat-Nasser S, Guo WG (2006) Superelastic and cyclic response of NiTi SMA at various strain rates and temperatures. Mech Mater 38(5–6):463–474. https://doi.org/10.1016/j.mechmat.2005.07.004

37. Yu C, Kang G, Song D, Kan Q (2015) Effect of martensite reorientation and reorientation-induced plasticity on multiaxial transformation ratchetting of super-elastic NiTi shape memory alloy: new consideration in constitutive model. Int J Plast 67:69–101. https://doi.org/10.1016/j.ijplas.2014.10.001

38. Milošev I, Kapun B (2012) The corrosion resistance of Nitinol alloy in simulated physiological solutions: Part 1: The effect of surface preparation. Mater Sci Eng, C 32(5):1087–1096. https://doi.org/10.1016/j.msec.2011.11.007

39. Shimoga G, Kim TH, Kim SY (2021) An intermetallic NiTi-based shape memory coil spring for actuator technologies. Metals 11(8):1212. https://doi.org/10.3390/met11081212

40. Kapoor D (2017) Nitinol for medical applications: a brief introduction to the properties and processing of nickel titanium shape memory alloys and their use in stents. Johns Matthey Technol Rev 61(1):66–76. https://doi.org/10.1595/205651317X694524

41. Fadlallah SA, El-Bagoury N, El-Rab SMG, Ahmed RA, El-Ousamii G (2014) An overview of NiTi shape memory alloy: corrosion resistance and antibacterial inhibition for dental application. J Alloy Compd 583:455–464. https://doi.org/10.1016/j.jallcom.2013.08.029

42. Nazarahari A, Canadinc D (2021) Prediction of the NiTi shape memory alloy composition with the best corrosion resistance for dental applications utilizing artificial intelligence. Mater Chem Phys 258:123974. https://doi.org/10.1016/j.matchemphys.2020.123974

43. Fang C, Cao C, Xiao Y, Zheng Y (2023) Effect of corrosion on self-centering energy dissipative devices. Eng Struct 293:116664. https://doi.org/10.1016/j.engstruct.2023.116664

44. Phukaoluan A, Srirussamee K, Khantachawana A, Chuchonak M, Tunthawiroon P (2024) Influence of the oxide film on the performance and corrosion resistance of TiNiCu shape memory alloys as the heat engine actuator. Eng Sci 31:1226. https://doi.org/10.30919/es1226

45. Delville R, Malard B, Pilch J, Sittner P, Schryvers D (2011) Transmission electron microscopy investigation of dislocation slip during superelastic cycling of Ni–Ti wires. Int J Plast 27(2):282–297. https://doi.org/10.1016/j.ijplas.2010.05.005

46. Ahadi A, Sun Q (2015) Stress-induced nanoscale phase transition in superelastic NiTi by in situ X-ray diffraction. Acta Mater 90:272–281. https://doi.org/10.1016/j.actamat.2015.02.024

47. Hua P, Xia M, Onuki Y, Sun Q (2021) Nanocomposite NiTi shape memory alloy with high strength and fatigue resistance. Nat Nanotechnol 16(4):409–413. https://doi.org/10.1038/s41565-020-00837-5

48. Hashemi YM, Kadkhodaei M, Mohammadzadeh MR (2019) Fatigue analysis of shape memory alloy helical springs. Int J Mech Sci 161:105059. https://doi.org/10.1016/j.ijmecsci.2019.105059

49. Nargatti K, Ahankari S (2022) Advances in enhancing structural and functional fatigue resistance of superelastic NiTi shape memory alloy: a review. J Intell Mater Syst Struct 33(4):503–531. https://doi.org/10.1177/1045389X211023582

50. Xiao Y, Zeng P, Lei L (2018) Micromechanical modeling on thermomechanical coupling of cyclically deformed superelastic NiTi shape memory alloy. Int J Plast 107:164–188. https://doi.org/10.1016/j.ijplas.2018.04.003

51. Xu L, Solomou A, Baxevanis T, Lagoudas D (2021) Finite strain constitutive modeling for shape memory alloys considering transformation-induced plasticity and two-way shape memory effect. Int J Solids Struct 221:42–59. https://doi.org/10.1016/j.ijsolstr.2020.03.009

52. Ardali A, Rouzegar J, Mohammadi S, Karimi M (2022) Transformation-induced plasticity in SMA composites experiencing fiber bridging phenomenon. Mater Sci Eng, A 858:144105. https://doi.org/10.1016/j.msea.2022.144105

53. Saab W, Racioppo P, Ben-Tzvi P (2019) A review of coupling mechanism designs for modular reconfigurable robots. Robotica 37(2):378–403. https://doi.org/10.1017/S0263574718001066

54. Wang X, Zhang M, Ge W (2016) A novel docking mechanism design and dynamic performance analysis of self-reconfigurable modular robot. In: Advances in reconfigurable mechanisms and robots II, Springer International Publishing, pp 681–692 https://doi.org/10.1007/978-3-319-23327-7_58

55. Delrobaei M, McIsaac KA (2009) Connection mechanism for autonomous self-assembly in mobile robots. IEEE Trans Rob 25(6):1413–1419. https://doi.org/10.1109/TRO.2009.2030227

56. Tosun T, Davey J, Liu C, Yim M (2016) Design and characterization of the ep-face connector. In: 2016 IEEE/RSJ international conference on intelligent robots and systems (IROS), IEEE, pp 45–51 https://doi.org/10.1109/IROS.2016.7759033

57. Ghazali FAM, Hasan MN, Rehman T, Nafea M, Ali MSM, Takahata K (2020) MEMS actuators for biomedical applications: a review. J Micromech Microeng 30(7):073001. https://doi.org/10.1088/1361-6439/ab8832

58. Moura TDO, Tsukamoto T, de Lima MDW, Tanaka S (2016) Hybrid MEMS-SMA structure for intraocular lenses. Sens Actuators, A 243:15–24. https://doi.org/10.1016/j.sna.2016.03.005

59. Xu J, Kimura Y, Tsuji K, Abe K, Shimizu T, Hasegawa H, Mineta T (2020) Fabrication and characterization of SMA film actuator array with bias spring for high-power MEMS tactile display. Microelectron Eng 227:111307. https://doi.org/10.1016/j.mee.2020.111307

60. Munasinghe KC, Bowatta BGCT, Abayarathne HYR, Kumararathna N, Maduwantha LKAH, Arachchige NMP, Amarasinghe YWR (2016) New MEMS based micro gripper using SMA for micro level object manipulation and assembling. In: 2016 Moratuwa engineering research conference (MERCon), IEEE, pp 36–41 https://doi.org/10.1109/MERCon.2016.7480112

61. Liu C, Yim M (2021) A quadratic programming approach to manipulation in real-time using modular robots. arXiv preprint arXiv:2104.02755. https://doi.org/10.48550/arXiv.2104.02755

62. Arora JS (2004) Introduction to optimum design. Elsevier, Amsterdam